2016

Selection Dynamics in the Germinal Center During Antibody Affinity Maturation

Alexander Gitlin

SELECTION DYNAMICS IN THE GERMINAL CENTER DURING ANTIBODY AFFINITY MATURATION

A Thesis Presented to the Faculty of

The Rockefeller University

in Partial Fulfillment of the Requirements for

the degree of Doctor of Philosophy

by

Alexander Gitlin

June 2016

SELECTION DYNAMICS IN THE GERMINAL CENTER DURING ANTIBODY AFFINITY MATURATION

Alexander Gitlin, Ph.D.

The Rockefeller University 2016

The maturation of antibody affinity during the immune response, discovered as a serological phenomenon in 1964, is critical to the development of high affinity humoral immunity. This process takes place in germinal centers (GCs), which are microanatomical structures composed of antigen-specific B lymphocytes that form in secondary lymphoid organs upon infection or immunization. High affinity B cells are selectively expanded in the GC by iterative rounds of migration between a zone of hypermutation and proliferation (the dark zone, or DZ) and a zone of selection (the light zone, or LZ). The mechanism whereby somatic antibody mutants are selected on the basis of affinity has been elusive.

In the first part of this thesis, I demonstrate that affinity-based selection in the GC operates through regulation of proliferation and hypermutation. B cells with affinity-enhancing mutations capture more antigen through their BCRs for presentation as peptide-MHCII to CD4+ T cells. In turn, enhanced T cell help induces selected B cells to return to the DZ, where they spend a prolonged period of time proliferating in between rounds of competition in the LZ. By dividing a greater number of times during each passage through the DZ, high

affinity cells can expand within the population and are provided more opportunities to hypermutate their antibody genes.

In the second part of this thesis, I examine the regulation of cell cycles in the DZ during GC selection. Transcriptional profiling revealed that T cell help enhanced signaling through the E2F and c-Myc pathways within selected GC B cells in the DZ. Moreover, T cell help increased the speed with which selected GC B cells progressed through both the S and G2/M phases. Genome sequencing and single-molecule analyses revealed that S phase is regulated by increasing the speed of DNA replication forks, while maintaining the dynamics of replication origin activation throughout the genome. Thus, T cells mediate affinity-based selection in the GC by inducing selected cells to reside longer in the DZ where they undergo accelerated cell cycles.

For their incredible support, love and friendship, I dedicate this thesis to my family – my dad, my mom, Karen, Jonathan, and Erin.

ACKNOWLEDGEMENTS

First, I would like to thank my advisor Michel Nussenzweig. Without his guidance and support, the work in this thesis would not have been possible. I cannot imagine having had an opportunity to spend these years in a better intellectual and scientific environment, nor can I imagine a better mentor than Michel.

I owe a great deal of thanks to many people: Ziv Shulman, my teammate on the germinal center, from whom I learned a great deal; Davide Robbiani and Mila Jankovic for reagents, advice, and discussion; Klara Velinzon and Neena Thomas for help with cell sorting; Lotta von Boehmer and Sarah Ackerman for antibody cloning; Connie Zhao and Bin Zhang for assistance with high throughput sequencing; Anna Gazumyan for antibody cloning and production; Alex Abadir, Cassie Liu, and Jovana Golijanin for antibody production; Scott Lowe, Nina Papavasiliou, Tomohiro Kurosaki, and Atsushi Miyawaki for mice; Amnon Koren for discussion and assistance with replication timing analysis; Thiago Oliveira for bioinformatics analyses; Tom Eisenreich, David Bosque, and Susan Hinklein for mouse colony management; Kai-Hui Yao for technical assistance; Mathew Jones for discussion and assistance with DNA fiber analyses; Qiao Wang and Natalia Freund for discussion; Christian Mayer for hands-on assistance with experiments; Hugo Mouquet and Johannes Scheid for discussion; Daniel Mucida for his continued support and advice;

Philipp Rommel, Ari Halper-Stromberg, Zander Nguyen, Andrew Levine, and Josh Horwitz for their continued friendship, camaraderie, and discussions; Zoran Jankovic for laboratory support; Virginia Menendez and Jennifer McQuillan for administrative assistance; Olaf Andersen, Ruthie Gotian, and the Tri-Institutional M.D.-Ph.D. program office for wonderful support, guidance and advice over the years; Jason Cyster for generously agreeing to travel from San Francisco to be the external examiner on my thesis committee; Nina Papavasiliou, Eric Pamer, and Sasha Rudensky for their service on my thesis committee. The Nussenzweig lab as a whole has been an immensely enjoyable place to work over the last few years, and I have all of the members, past and present, to thank for this.

This work was supported by NIH MSTP grant T32GM07739, NIAID grant 1F30AI109903-01, NIH grants AI037526-19 and AI072529-06, the NIH Center for HIV/AIDS Vaccine Immunology and Immunogen Discovery (CHAVI-ID) 1UM1 AI100663-01, and the Howard Hughes Medical Institute.

Finally, I want to thank my family. My wife Erin has been my best friend, my closest confidante, my love, and my partner. My father Daniel, my mother Silvia, and my siblings, Jonathan and Karen, have continually given me their unconditional support, encouragement, advice, and love. I

cannot thank them enough for all they have given me over the past few years.

TABLE OF CONTENTS

LIST OF FIGURES

CHAPTER 1:

INTRODUCTION

1.1 Secondary antibody diversification

The adaptive immune system protects vertebrates from pathogens with a limitless array of microbial structures. How the immune system accomplishes this feat was presciently envisioned by the clonal selection theory, proposed more than 50 years ago (Burnet, 1959; Talmage, 1959). According to this theory, lymphocytes are diverse, with each individual cell bearing a unique receptor that triggers the expansion of that clone when bound by antigen. In the ensuing decades, the basic tenets of clonal selection theory proved correct, and T and B lymphocytes emerged as the primary effector cells of this system (Gitlin and Nussenzweig, 2015).

The primary repertoire of B cell antigen receptors (BCRs) is generated during the development of B cells in the bone marrow by V(D)J recombination (Hozumi and Tonegawa, 1976; Tonegawa, 1983). In this process, the antigen-binding variable region of the immunoglobulin gene is assembled by recombination of a large pool of potential gene segments. Yet, a major drawback of this system is that antibodies with specificity for self-antigens are generated at significant frequencies (Meffre et al., 2000; Rajewsky, 1996; Wardemann et al., 2003). These potentially deleterious specificities must therefore be removed from the

repertoire by clonal deletion (Hartley et al., 1991; Nemazee and Burki, 1989; Russell et al., 1991; Wardemann et al., 2003), receptor editing (Casellas et al., 2001; Gay et al., 1993; Tiegs et al., 1993), or functional anergy (Goodnow et al., 1988; Goodnow et al., 1989; Zikherman et al., 2012). B cells that successfully complete these tasks go on to mature and circulate within the blood and lymphoid organs bearing BCRs composed of surface immunoglobulin and the Ig-alpha/beta heterodimer.

Binding of the BCR by antigen induces specific B cells to clonally expand, differentiate and secrete their antibody molecules. Whereas the N-terminal variable region of the antibody recognizes the antigen, the C-terminal constant region (Fc) engages the effector arm of the immune system by binding Fc receptors on innate immune cells (Pincetic et al., 2014). However, germline-encoded antibodies are often low in affinity and the Fc domains of the antibodies of naïve B cells (immunoglobulin (Ig)M) possess limited effector function, requiring that antibodies be improved during immune responses. Secondary antibody diversification meets these demands in a process not originally foreseen by clonal selection theory.

1.2 Affinity maturation

The possibility that antigen-specific antibodies change during immune responses can be traced, in part, to the discovery of the affinity maturation phenomenon. In

their initial discovery of this phenomenon, Eisen and Siskind found that immunization with T cell-dependent antigens elicited serum antibodies that underwent progressive increases in affinity over time (Eisen and Siskind, 1964). Hybridoma technology and antibody gene sequencing subsequently demonstrated the basis of affinity maturation: antigen-specific B cells hypermutate their variable regions and affinity-enhancing mutations are positively selected (Berek and Milstein, 1987; McKean et al., 1984; Weigert et al., 1970). Moreover, to provide antibodies with enhanced effector function, B cells undergo class switch recombination (CSR), thereby exchanging the constant region of IgM with that of the immunoglobulin G, E, or A class (Stavnezer et al., 2008). Thus, CSR, somatic hypermutation (SHM), and affinity-based selection together generate high affinity class-switched antibodies that confer protective humoral immunity onto the host.

The workings of secondary diversification and selection of antibodies were further elucidated by the discovery that these processes occur in the germinal center (GC) (Berek et al., 1991; Jacob et al., 1991b). The events during the B cell response that culminate in the mature GC unfold in a stereotyped manner (Allen et al., 2007a; Victora and Nussenzweig, 2012). Following their activation, antigen-specific B and T cells migrate to the border that segregates their respective zones in secondary lymphoid organs (Garside et al., 1998; Jacob et al., 1991a; Liu et al., 1991; Okada et al., 2005; Schwickert et al., 2011). This ordered process of migration is reciprocally mediated by the chemokine

receptors CXCR5 and CCR7: activated B cells are attracted to the T cell zone by upregulation of CCR7, while T cell migration toward the B cell follicle is driven by upregulation of CXCR5 and downregulation of CCR7 (Reif et al., 2002). Within the T/B border region, B cells receive help from cognate CD4+ T cells as the B cells proliferate, class switch and differentiate into antibody-secreting plasmablasts, memory B cells or GC B cells. Interclonal competition among antigen-specific B cells begins at the this stage, ensuring that only B cells with relatively higher affinity germline-encoded antibodies will enter the GC and plasmablast compartments (Dal Porto et al., 2002; Paus et al., 2006; Schwickert et al., 2011; Shih et al., 2002a).

As the extrafollicular phase of the response subsides, the mature GC persists within the follicle (Jacob et al., 1991a). GC B cells continue to proliferate at high rates, with cell cycle durations estimated between 6 and 12 hours (Allen et al., 2007b; Hauser et al., 2007), and express the enzyme activation-induced cytidine deaminase (AID), which induces both SHM and CSR (Muramatsu et al., 2000; Muramatsu et al., 1999; Revy et al., 2000). AID deaminates cytidine residues to produce uridine in the variable and switch regions of the antibody gene (Bransteitter et al., 2003; Chaudhuri et al., 2003; Dickerson et al., 2003; Pham et al., 2003; Ramiro et al., 2003; Sohail et al., 2003). The resulting U-G mismatches are then recognized by the DNA repair machinery and can be processed in an error-prone manner to generate mutations or double-strand DNA breaks, leading to SHM and CSR, respectively (Di Noia and Neuberger, 2007; Peled et al.,

2008). Remarkably, the rate of SHM exceeds the normal mutation rate of the genome by approximately one million-fold, as ~1 somatic mutation in the antibody gene is introduced per 10^3 base pairs during each cell cycle (McKean et al., 1984). This high rate of antibody mutation allows antibody affinity to rise dramatically above what is encoded in the germline, enabling rapid and potent antibody responses against an unlimited variety of pathogens, even those which humans have only been exposed to in our most recent evolutionary history.

1.3 Germinal center organization and dynamics

The GC is a highly organized microanatomical structure, composed of two poles – a light (LZ) and dark (DZ) zone (Nieuwenhuis and Opstelten, 1984). Distinct cell types occupy the DZ and LZ and help mediate the activities contained therein. For example, in addition to B cells, the LZ is occupied by follicular dendritic cells (FDCs) that retain antigen on their surface in the form of immune complexes and a specialized subset of antigen-specific CD4+ T cells known as T follicular helper (T_{FH}) cells (Allen et al., 2007a; Mandel et al., 1980; Mandel et al., 1981; Victora and Nussenzweig, 2012). In contrast, the DZ contains a far lower density of T_{FH} cells and is instead occupied by mitotically active GC B cells that express high levels of AID. Over time, high affinity GC mutants emerge by positive selection and eventually exit the GC as memory B cells and plasma cells (Victora and Nussenzweig, 2012).

The segregation of antigen in the LZ and proliferation in the DZ requires that GC cells exchange between these two zones. Interzonal migration in the GC was first suggested by nucleotide-labeling studies, which indicated that dividing DZ cells become visible in the LZ over time (Hanna, 1964). Based on these studies, mathematical simulations suggested that the efficiency of affinity maturation could be achieved in an iterative fashion, by recycling only those cells that are selected in the LZ for another round of mutation and division in the DZ – an idea known as the cyclic re-entry model (Kepler and Perelson, 1993; Oprea and Perelson, 1997). More recently, intravital multiphoton microscopy directly visualized the bidirectional nature of movement of GC cells between LZ and DZ (Allen et al., 2007b; Hauser et al., 2007; Schwickert et al., 2007). However, whether interzonal migration involves equal bidirectional movement, or whether movement of GC cells is polarized from one zone to the other as predicted by the cyclic re-entry model, remained unclear.

To test this idea, our laboratory previously developed a transgenic mouse expressing a photoactivatable green fluorescent protein (PAGFP) (Patterson and Lippincott-Schwartz, 2002; Victora et al., 2010). This system allowed DZ or LZ B cells to be labeled with a high degree of spatial precision by selectively photoactivating either zone by two-photon irradiation (Victora et al., 2010). GC B cells labeled in this fashion were then tracked over long periods of time, revealing the existence of a net vector of movement from DZ to LZ, with nearly 50% of DZ cells migrating to the LZ but only 10% of LZ cells migrating to the DZ within 6

hours. Furthermore, consistent with the idea that distinct cellular activities take place in the LZ and DZ, genes associated with cellular activation were upregulated in the LZ, while cell cycle-associated genes were highly expressed in the DZ.

GC organization and migration are mediated by the chemokine receptors CXCR4 and CXCR5 (Allen et al., 2004; Allen et al., 2007a). For example, CXCR4 deficient cells in an otherwise normal GC are absent from the DZ, whereas CXCR5 deficiency leads to disorganized GCs devoid of discernible zones. Furthermore, the ligands for these receptors are zonally polarized: CXCL12 (the ligand for CXCR4) is produced by reticular cells in the DZ, while CXCL13 (the ligand for CXCR5) is present in the LZ (Allen et al., 2004; Allen et al., 2007a; Bannard et al., 2013). These findings have led to a model whereby LZ cells migrate to the DZ by upregulating CXCR4, while CXCR4 downregulation allows CXCR5 to guide migration to the LZ.

Although positioning of GC cells in the LZ and DZ coincides with distinct cellular states, local cues in the DZ are not required to induce a DZ-like state or for GC cells to undergo activities normally associated with the function of the DZ (Bannard et al., 2013). Namely, CXCR4-deficient GC B cells, which remain in the LZ, still proliferate at near-normal levels and undergo SHM, albeit at a lower rate. Therefore, the transition between DZ and LZ states is independent of physical positioning in the GC and is thus a cell-intrinsic feature of GC B cells.

Nevertheless, the parameters that govern the DZ/LZ transition remain largely undefined.

1.4 Mechanism of affinity-based selection

In order for affinity-based selection to take place, higher and lower affinity GC B cells must compete, such that only higher affinity cells receive signal(s) that mediate their selective expansion. Two non-mutually exclusive possibilities have long been considered as the basis for this competition (Allen et al., 2007a; MacLennan, 1994; Victora and Nussenzweig, 2012). First, because of the presence of antigen in the LZ, high affinity BCRs might transduce an antigen-mediated signal that differs from that of a lower affinity BCR. Secondly, high affinity BCRs can endocytose more antigen and thereby elicit more help from T cells by presenting a higher density of surface peptide-major histocompatibility class II complexes (pMHCII). However, because both of these signals are downstream of the BCR and are therefore inherently linked to one another, experimentally testing whether BCR signaling or T cell help mediate selection was a major challenge.

1.4.1 Role of the BCR in selection

Upon engagement by antigen, the signal transducing component of the BCR, the Ig-alpha/Ig-beta heterodimer, initiates signaling through immune receptor

tyrosine activation motifs (ITAMs) (Hermanson et al., 1988; Hombach et al., 1990; Reth, 1989; Sakaguchi et al., 1988; Sanchez et al., 1993; Shaw et al., 1990; Williams et al., 1994). Src and Syk family kinases phosphorylate ITAMs, thereby providing a platform that mediates a cascade of phosphorylation events by other SH2-domain containing kinases (Craxton et al., 1999; Gauld et al., 2002; Kurosaki, 1999; Reth and Wienands, 1997). As a result, several downstream signaling pathways are activated, including the NFAT, PI3K, NF-κB and MAPK pathways (Kurosaki et al., 2010).

B cells undergo continuous BCR-mediated selection (Meffre et al., 2000; Rajewsky, 1996). Beginning in development, those cells unable to produce an immunoglobulin heavy chain, and thus unable to produce a pre-BCR, fail to develop past the pro-B cell stage (Gu et al., 1993; Kitamura et al., 1992; Kitamura and Rajewsky, 1992; Kitamura et al., 1991). Similarly, B cell development is severely impeded by interference with the expression or function of Ig-alpha or Ig-beta (Gong and Nussenzweig, 1996; Torres et al., 1996).

Mature B cells that complete development continue to maintain a requirement for the BCR to survive. For example, conditional genetic ablation of surface immunoglobulin on mature B cells leads to their rapid apoptotic demise (Lam et al., 1997). However, this survival requirement for the BCR is not simply a structural one that involves the assembly and/or surface expression of the BCR. Rather, B cells require continuous “tonic” signals from the BCR, since conditional

removal of the cytoplasmic tail of Ig-alpha, thereby leaving a signaling-deficient BCR expressed on the cell surface, leads to rapid B cell death as well (Kraus et al., 2004). Strikingly, the survival of “receptorless” B cells can be rescued by constitutive activation of the PI3K pathway, revealing a key role for this pathway in mediating continual BCR-dependent survival of mature B cells (Srinivasan et al., 2009).

Whereas the above-described roles of the BCR in survival are independent of immunizing antigen, the BCR plays an antigen-dependent role in selection during immune responses. The antibody response is initiated when mature B cells encounter antigen, which can occur via several routes (Harwood and Batista, 2010). Smaller antigens (<70 kDa) diffuse into the B cell follicles across the subcapsular sinus (SCS) of lymph nodes (Pape et al., 2007). Alternatively, a system of conduits that permeate the follicles can also deliver small antigens to B cells (Roozendaal et al., 2009). By contrast, larger antigens like immune complexes, microbial pathogens, or particulate antigens accumulate at the SCS on the surface of locally resident macrophages (Carrasco and Batista, 2007; Junt et al., 2007; Phan et al., 2007). From this location, follicular B cells can acquire antigen and transport it to FDCs, where it persists for long periods of time to allow progressive, antigen-driven selection of high affinity BCRs in the GC.

The role of BCR signaling in GC selection remains elusive (Victora and Nussenzweig, 2012). Early work found that limiting amounts of immunizing

antigen produced a greater degree of affinity maturation, suggesting a potential role for antigen during selection (Eisen and Siskind, 1964; Goidl et al., 1968; Nussenzweig and Benacerraf, 1967). However, direct studies of the BCR/antigen interaction in the GC have been hampered by the complex nature of antigen on FDCs. For example, acute injection of soluble antigen to ongoing immune responses leads to apoptosis and the dissolution of the GC (Han et al., 1995b; Pulendran et al., 1995; Shokat and Goodnow, 1995; Victora et al., 2010). Furthermore, when FDCs lack complement receptors that bind immune complexes, affinity maturation, though impaired, can still occur (Boes et al., 1998; Chen et al., 2000; Hannum et al., 2000; Matsumoto et al., 1996; Wu et al., 2000). Moreover, genetic deletion of various components of BCR signaling often lead to impaired or absent GC responses, obscuring whether these components play a role in selection (Victora and Nussenzweig, 2012). Finally, it has been suggested that BCR signaling is actively dampened in the GC by high levels of phosphatase activity (Khalil et al., 2012).

In order for BCR/antigen binding to mediate selection, higher affinity GC cells would have to prevent access of lower affinity cells to antigen on FDCs. However, intravital imaging has found that this is not the case: GC B cell interactions with FDCs displaying antigen are highly dynamic and rarely involve prolonged interactions that might allow discrimination among higher and lower affinity BCRs (Allen et al., 2007b; Hauser et al., 2007; Schwickert et al., 2007). Thus, a direct role for BCR signaling in the GC remains to be defined.

1.4.2 Role of T cell help in selection

T_{FH} cells enter the GC and are retained there by virtue of their expression of CXCR5 and sphingosine-1-phosphate receptor 2 (S1PR2) (Ansel et al., 1999; Haynes et al., 2007; Moriyama et al., 2014). These cells are underrepresented relative to GC B cells and are essential for the GC response. For example, T cell-deficient mice do not form GCs (Jacobson et al., 1974), and T cell-independent responses can form only transient, abortive GCs (de Vinuesa et al., 2000). T cells are also important for the maintenance of established GCs, since antibodies that perturb the CD40/CD40 ligand (CD40L) pathway lead to acute GC dissolution (Han et al., 1995a). Consistent with these findings, human patients with mutations in either CD40 or CD40L cannot form GCs and are thus susceptible to opportunistic infections due to a lack of high affinity, class-switched antibodies (Allen et al., 1993; Ferrari et al., 2001).

Various lines of evidence have suggested that T cell help might play a role in selection. For example, antigen presentation is highly sensitive to BCR affinity. In vitro, BCR/antigen affinities with K_d values ~ 10^{-6} have been found to be minimally required to detectably trigger T cell responses. Above this threshold, antigen presentation rises with affinity until reaching a ceiling of K_d ~ 10^{-10}, at which point internalization and degradation of antigen occurs more rapidly than dissociation of antigen from the BCR (Batista and Neuberger, 1998, 2000).

Consistent with the sensitivity of antigen presentation to BCR affinity, T cells preferentially synapse with B cells displaying higher surface densities of pMHCII in vitro (Depoil et al., 2005). However, in vivo, the majority of interactions between GC B cells and T_{FH} cells are short-lived and therefore likely unproductive, raising the possibility that GC B cells compete for limiting amounts of help from T_{FH} cells (Allen et al., 2007b).

To examine this issue directly, our laboratory used the DEC205 lectin as an antigen-delivery tool. DEC205 was originally described as the target of an antibody clone (NLDC-145) that primarily recognized dendritic cells (Kraal et al., 1986). This type-I transmembrane protein is homologous to the macrophage mannose receptor and carries a cytoplasmic domain that mediates endocytosis. Accordingly, targeting DEC205 with an antibody leads to internalization and delivery to multivesicular endosomal compartments involved in processing antigen for presentation on MHCII (Jiang et al., 1995). More recently, high levels of DEC205 expression were documented on activated B cells as well (Kamphorst et al., 2010; Victora et al., 2010).

To utilize DEC205 to examine T cell help, GCs were induced using a prime-boost immunization protocol and were composed of: (1) immunoglobulin knock-in B cells ($B1\text{-}8^{hi}$) with specificity for the chemical hapten 4-hydroxy-3-nitrophenylacetyl (NP) and (2) endogenous ovalbumin (OVA)-specific T cells (Schwickert et al., 2007; Shih et al., 2002b). Critically, a minor subset of the B1-

8^{hi} GC B cells were $DEC205^{+/+}$ (~15%), whereas the majority were $DEC205^{-/-}$ (~85%) (Victora et al., 2010). During GC responses induced in this fashion, pMHCII levels were acutely increased among the B1-8^{hi} $DEC205^{+/+}$ GC B cells by injecting anti-DEC205 antibody fused at its C-terminus to OVA (αDEC-OVA). Delivering antigen in this fashion bypassed the BCR while providing the targeted subset of B1-8^{hi} $DEC205^{+/+}$ GC B cells with greater T cell help. These experiments demonstrated that increasing pMHCII levels suffices to induce selective expansion of B cells in the GC, providing direct evidence that T cell help is the limiting and crucial factor during selection.

1.4.3 T cell-mediated regulation of GC dynamics

A striking finding in the experiments described above was that T cell help altered the LZ/DZ distribution of selected B cells as they underwent expansion (Victora et al., 2010). Although B1-8^{hi} $DEC205^{+/+}$ GC B cells receiving increased T cell help were retained in the LZ 12 hours after αDEC-OVA injection, these B cells accumulated disproportionately (>90%) in the DZ over the ensuing 36 hours. Yet under normal circumstances, DZ cells migrate rapidly to the LZ, raising the question of how so many DZ cells might be accumulating during selection. One possibility is that T cell-mediated selection in the LZ leads to shuttling of GC cells to the DZ, whereas such migration events otherwise occur with lesser frequency. Secondly, receipt of selecting T cell help might lead to preferential survival of cells that would otherwise die in the DZ. Thirdly, the magnitude of T cell help

might regulate the length of time that GC B cells spend in the DZ, causing cells that are selected following αDEC-OVA treatment to disproportionately accumulate in the DZ, as observed experimentally. In this thesis, I examined the role of T cell help in regulating the dynamics of GC B cells during their selective expansion (Gitlin et al., 2014).

Chapter 2:

T cell help regulates proliferation and hypermutation in the germinal center

2.1. Role of antigen presentation in germinal center selection

I first asked whether the amount of antigen that B cells internalize regulates the degree of their expansion in the GC. I therefore used antibodies targeting DEC205 to deliver graded amounts of additional antigen to GC B cells (Jiang et al., 1995; Kamphorst et al., 2010; Victora et al., 2010). GCs were induced by priming mice intraperitoneally with the protein antigen ovalbumin (OVA), followed by adoptive transfer of B1-8^{hi} immunoglobulin heavy chain knock-in B cells, which are specific for NP when paired with the endogenous lambda light chain (Igλ), and subcutaneous boosting with OVA coupled to the hapten 4-hydroxy-3-nitrophenylacetyl (NP-OVA) (Schwickert et al., 2007; Shih et al., 2002a; Shih et al., 2002b).

To examine clonal expansion among B cells receiving differing amounts of antigen, mice received a mixture of B1-8^{hi} DEC205$^{+/+}$ and B1-8^{hi} DEC205$^{-/-}$ B cells at a 5:95 ratio prior to boosting. During the ongoing GC response, cognate OVA antigen was then delivered to DEC205$^{+/+}$ GC B cells in graded amounts

using chimeric DEC205 antibody (αDEC-OVA, Figure 2.1A). The maximal antigen dose administered (10 μg of αDEC-OVA) produced rapid and robust expansion of the B1-8^{hi} DEC205$^{+/+}$ GC B cells (Figure 2.1B and C). Lesser antigen doses, delivered by mixing αDEC-OVA with a chimeric αDEC205 antibody fused to an irrelevant control antigen *Plasmodium Falciparum* circumsporozoite protein (αDEC-CS) (Boscardin et al., 2006), caused the B1-8^{hi} DEC205$^{+/+}$ GC B cells to expand but to a lesser extent, in proportion to the dose of αDEC-OVA administered (Figure 2.1B and C).

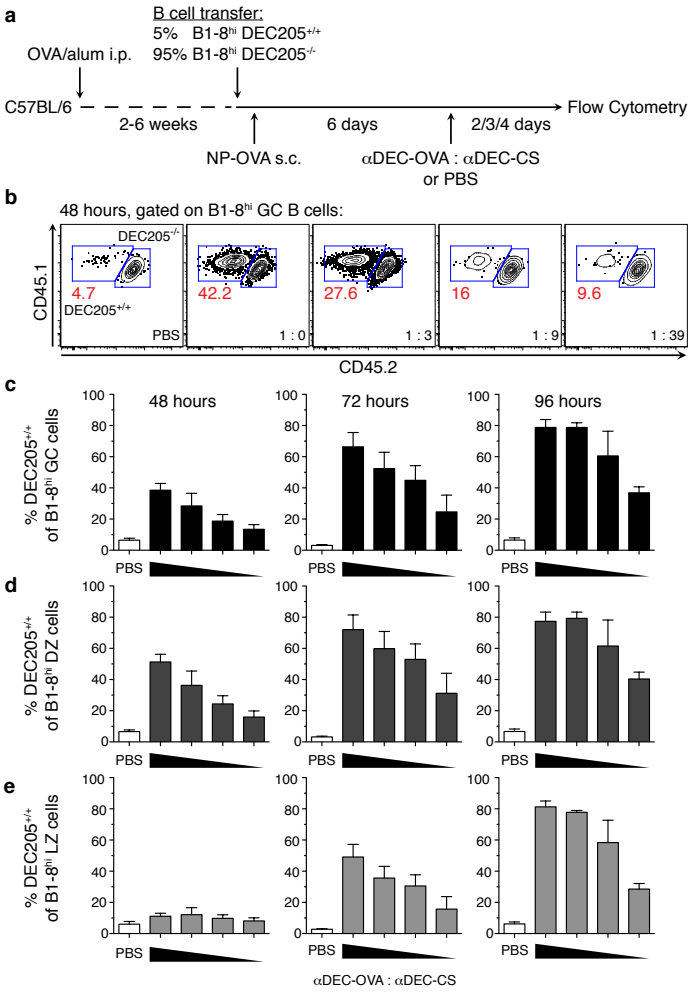

Figure 2.1. The amount of antigen presented by GC B cells regulates their expansion. a, Experimental protocol used for **1b-e**. Wild-type mice were primed by intraperitoneal immunization with OVA in alum. Two to six weeks later, mice received 1.5-5 x 10^6 B1-8^{hi} DEC205$^{+/+}$ and B1-8^{hi} DEC205$^{-/-}$ B cells at a 5:95 ratio and were boosted with NP-OVA. On day 6 after the boost, mice were injected with PBS or αDEC-OVA mixed with αDEC-CS at ratios of 1:0, 1:3, 1:9, or 1:39. Popliteal lymph node cells were analyzed 2, 3, and 4 days later by flow cytometry. **b,** Plots showing increased expansion of B1-8^{hi} DEC205$^{+/+}$ over B1-8^{hi} DEC205$^{-/-}$ GC B cells with increasing amounts of αDEC-OVA. **c-e,** Fraction of DEC205$^{+/+}$ B cells among total B1-8^{hi} GC B cells (**c**) or among B1-8^{hi} DZ (**d**) or LZ cells (**e**). Error bars = SEM. Data represent 2-3 independent experiments at each time point with a total of 4-6 mice per condition for all time points.

At 48 hours after chimeric antibody injection, the dose-dependent expansion of B1-8^{hi} DEC205$^{+/+}$ GC B cells could be seen in the DZ and only became apparent in the LZ at later time points (Figure 2.1D and E). This is in agreement with the idea that pMHCII-mediated selection occurs in the LZ and that clonal expansion takes place in the DZ (Victora et al., 2010). Importantly, increasing antigen presentation by the B1-8^{hi} DEC205$^{+/+}$ GC B cells also led to a dose-dependent numerical contraction of the B1-8^{hi} DEC205$^{-/-}$ GC B cell population (Figure 2.2). Thus, GC B cells that present increasing amounts of cognate antigen to T_{FH} cells selectively and proportionally expand within the GC population at the expense of GC B cells that present lesser amounts of antigen.

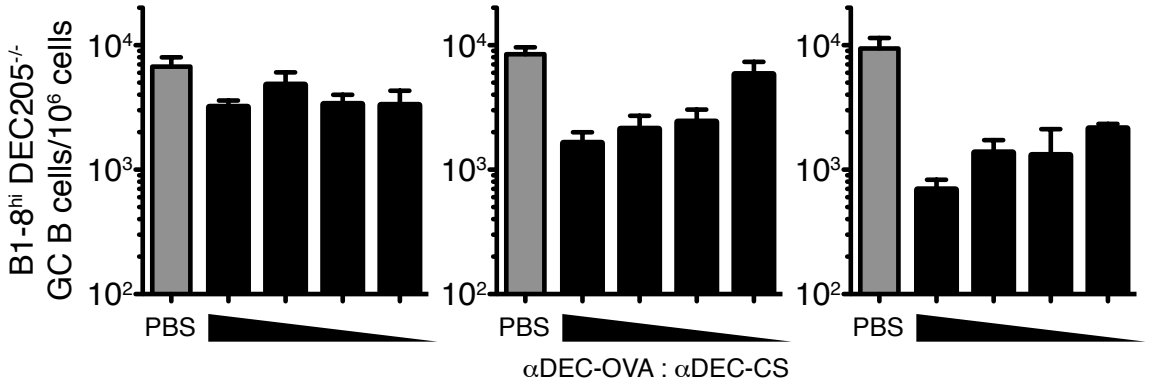

Figure 2.2. Selective expansion of B1-8^{hi} DEC205$^{+/+}$ GC cells involves contraction of B1-8^{hi} DEC205$^{-/-}$ GC cells. Total number of B1-8^{hi} DEC205$^{-/-}$ GC B cells per 10^6 lymph node cells from the experiment reported in Figure 2.1. Popliteal lymph node cells were analyzed 2 (left), 3 (middle), and 4 (right) days later by flow cytometry. Bars represent mean values; error bars = SEM.

2.2 Role of proliferation in affinity-based selection

B cells presenting more antigen could expand within the GC population by undergoing less cell death and/or by proliferating more than their competitors. In order to examine this issue mechanistically, I therefore sought to measure proliferation in the GC. Conventional methods of measuring cell division include the use of nucleotide labeling, DNA content stains, and dye-based dilution methods. Nucleotide labels and DNA content stains provide information on the fraction of cells distributed among the different cell cycle stages at a given moment. These means of cell cycle analyses therefore cannot provide dynamic information, such as the number of divisions a cell has undergone over time, due to two key reasons: (1) variability in the length of time required to progress through each cell cycle phase and (2) the asynchronous nature of unperturbed cell populations in vivo. Alternatively, cell cycle dyes like carboxyfluorescein succinimidyl ester (CFSE) dilute with mitosis, allowing direct enumeration of the number of times a cell population has divided. However, this method is unsuitable in the context of the GC because B cells proliferate and dilute these dyes before forming GCs (Schwickert et al., 2011).

To overcome this issue, we employed a system used by developmental biologists that involves dilution of a genetically encoded fluorescent protein to analyze proliferation dynamics (Tumbar et al., 2004). In this bi-transgenic system, a Vav

promoter drives expression of the tetracycline transactivator (tTA) protein, while a Doxycycline (DOX)-regulated promoter integrated in the endogenous Col1A1 locus drives expression of a histone H2B-mCherry fusion protein (tTA-H2B-mCh, Figure 2.3A) (Egli et al., 2007; Wiesner et al., 2005). At steady state, hematopoietic cells express tTA, which induces high levels of H2B-mCh expression (Figure 2.3B). DOX administration represses further tTA-mediated expression of H2B-mCh, allowing divisions that occur during DOX administration to dilute the mCherry signal.

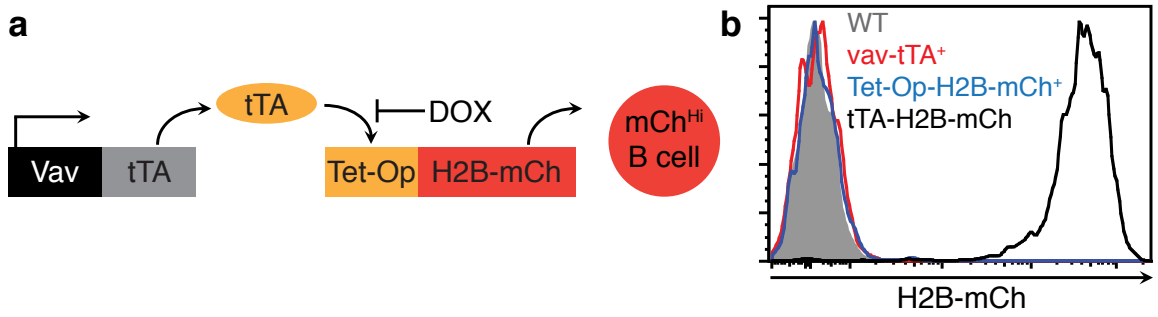

Figure 2.3. The tTA-H2B-mCh system a, The tTA protein is expressed from the Vav promoter, which directs synthesis of the H2B-mCherry fluorescent protein. H2B-mCh expression can be repressed by DOX. **b,** Histogram showing H2B-mCh fluorescence in $B220^{+}$ peripheral blood lymphocytes in wild-type (WT, gray), Vav-tTA^{+} (red), Tet-Op-H2B-mCh^{+} (blue), and tTA-H2B-mCh (black) mice.

To test if tTA-H2B-mCh can be used to follow proliferation of antigen-specific GC B cells, the prime-boost experiments described above were repeated using B1-8^{hi} tTA-H2B-mCh B cells. Follicular B cells, which rarely proliferate, did not dilute H2B-mCh after DOX treatment. In contrast, GC B cells diluted H2B-mCh after 36 hours of DOX treatment, generating a spectrum of H2B-mCh expression that

included discrete peaks corresponding to cell divisions. By 84 hours, GC B cells had completely diluted H2B-mCh (Figure 2.4).

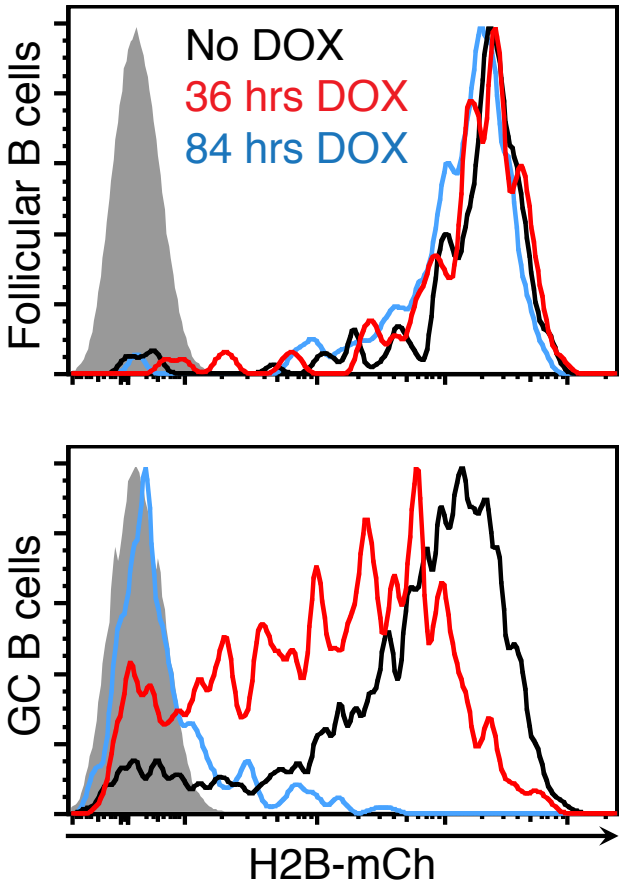

Figure 2.4. Using the tTA-H2B-mCh system to analyze GC B cell division. Histograms show H2B-mCh expression in B1-8^{hi} tTA-H2B-mCh B cells in the follicular (upper) and GC (lower) compartment of mice that were given DOX for 36 hours (red), 84 hours (blue), or untreated (black). Solid gray represents non-fluorescent B cells in the indicated compartment.

To further confirm that H2B-mCh dilution reflects bona fide cell divisions, purified splenic B cells from tTa-H2B-mCh mice were labeled with CFSE and cultured with lipopolysaccharide (LPS) and interleukin (IL)-4. After 72 hours, gating on progressively lower H2B-mCh levels revealed that these cells had indeed divided

a proportional number of times. We conclude that the tTA-H2B-mCh can be used to monitor GC B cell proliferation dynamics.

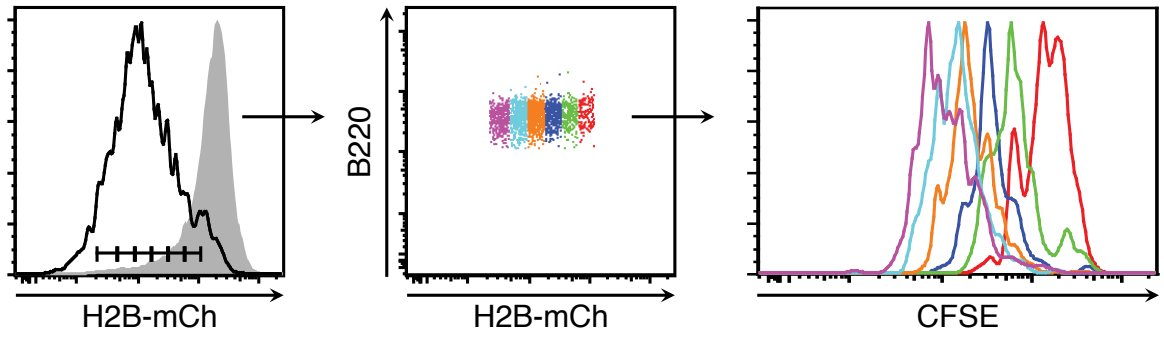

Figure 2.5. H2B-mCh dilution reflects bona fide cell division. Left, Purified splenic B cells from tTA-H2B-mCh mice were labeled with CFSE and stimulated with LPS and IL-4 in culture for 0 or 72 hours (gray and black, respectively). Middle, Color-coded H2B-mCh gates after 72 hours in culture. Right, Histogram displaying CFSE levels for the color-coded H2B-mCh gates.

To determine whether T cell help controls the number of cell cycles GC B cells undergo, I delivered additional antigen to GC B cells using αDEC-OVA. After 60 hours on DOX, B1-8^{hi} DEC205$^{+/+}$ tTA-H2B-mCh GC B cells from control mice, treated with either αDEC-CS or PBS, were nearly evenly distributed among mCh^{Med}, ^{Lo}, and $^{-}$ groups, representing cells that had progressively divided a greater number of times (Figure 2.6). In contrast, in the same timeframe, αDEC-OVA induced selection caused ~50% of targeted GC B cells to become mCh^{-} while ~40% became mCh^{Lo}. Thus, increased T cell help leads to a greater number of cell divisions by GC B cells undergoing selective expansion.

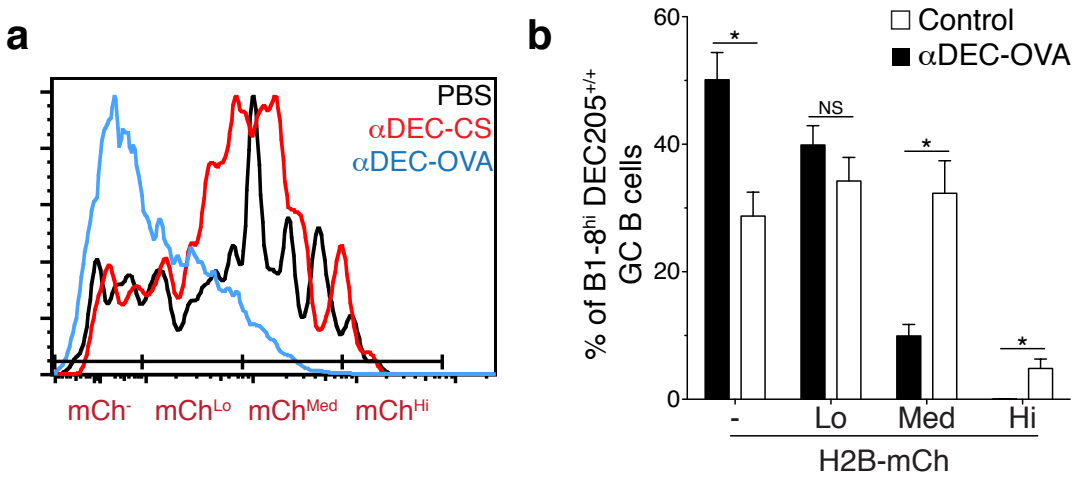

Figure 2.6. T cell help regulates the number of GC B cell divisions. a, Histogram displaying H2B-mCh expression in B1-8^{hi} tTA-H2B-mCh GC B cells in mice receiving a 5:95 mixture of B1-8^{hi} tTA-H2B-mCh and B1-8^{hi} DEC205$^{-/-}$ B cells and treated with either PBS (black), αDEC-CS (red), or αDEC-OVA (blue) for 72 hours and administered DOX for 60 hours prior to flow cytometry. **b,** Bar graph represents mean fraction of B1-8^{hi} tTA-H2B-mCh GC B cells in the gates displayed in **a**. Data represent 3 experiments with 2-3 mice per condition in each experiment. * $p<0.005$, two-tailed Mann-Whitney test.

Concomitant with the increased number of cell divisions, selectively expanding GC B cells were altered in their LZ/DZ distribution (Figure 2.7). Control cells were found in the DZ and LZ at a ~2:1 ratio, while αDEC-OVA targeted GC B cells were nearly exclusively in the DZ (~90%).

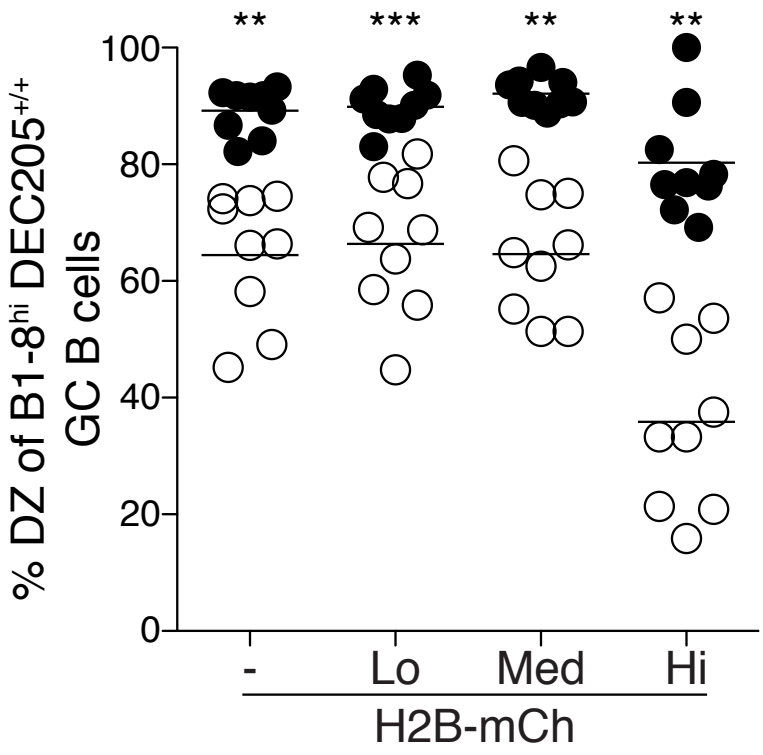

Figure 2.7. T cell help shifts LZ/DZ distribution of selected GC B cells. Percent of B1-8^{hi} tTA-H2B-mCh GC B cells with a DZ phenotype within the H2B-mCh gates displayed in Figure 2.6A. ** $p < 0.001$; *** $p < 0.0001$, two-tailed Mann-Whitney test.

2.3. Dynamic regulation of interzonal migration in the germinal center

To examine cell cycle dynamics and their regulation during selection, I used a double-nucleoside pulse method. For this purpose, GC B cells were labeled with an intravenous pulse of 5-ethynyl-2′-deoxyuridine (EdU) followed 1 hour later by 5-bromo-2′-deoxyuridine (BrdU), which are incorporated into the DNA of cells that are in S phase at the time of injection. This method allows GC B cells to be identified at various stages of DNA replication: early ($EdU^{-}BrdU^{+}$), mid/late

(EdU^{+}BrdU^{+}) and post- (EdU^{+}BrdU^{-}) S phase periods of the cell cycle (Figure 2.8).

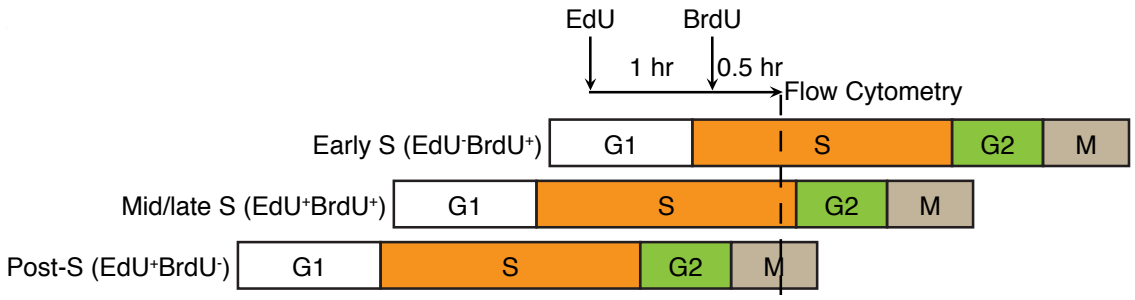

Figure 2.8. EdU/BrdU labeling strategy to examine S phase dynamics in the GC. Mice with ongoing GCs were injected intravenously with EdU followed 1 hour later by BrdU. Flow cytometry was performed a half-hour after BrdU administration. Early S phase cells incorporate only the second nucleotide analog and are thus EdU^{-}BrdU^{+}. Mid/late S phase cells incorporate both nucleotide analogs and are therefore EdU^{+}BrdU^{+}. Post-S phase cells that completed S phase in between the two pulses are EdU^{+}BrdU^{-}.

Under control conditions, GC B cells in early and mid/late-S phases were in both LZ and DZ; post-S phase cells were mainly in the DZ (Figure 2.9). This finding is consistent with the notion that GC B cells can initiate S phase in the LZ and then migrate to the DZ to complete the cell cycle. Moreover, the ~2:1 DZ:LZ ratio of early S phase cells suggests that, once in the DZ, GC B cells can initiate two additional cell divisions on average. In contrast, inducing selection with αDEC-OVA shifted early S phase cells to the DZ (~86%), while fewer early S phase cells among non-selected B1-8^{hi} DEC205$^{-/-}$ cells were in the DZ (59%). I conclude

that increasing the amount of antigen presented to T_{FH} cells increases the proportion S phase initiation events that take place in the DZ.

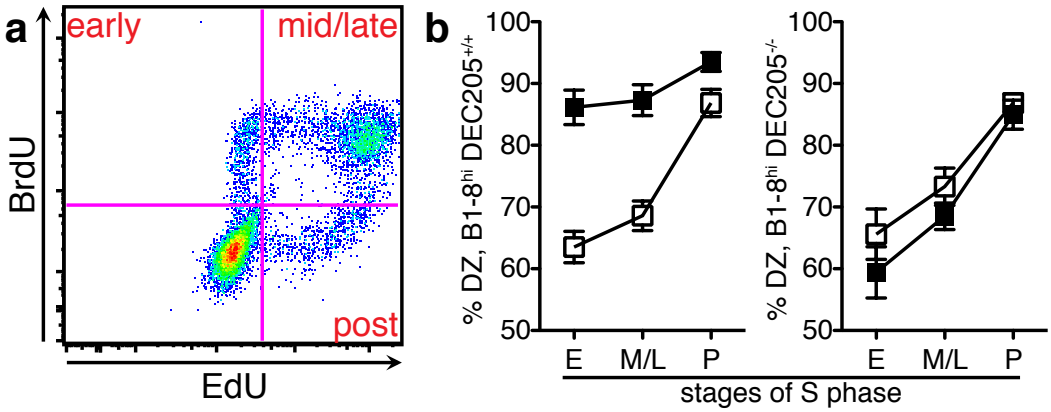

Figure 2.9. T cell-mediated selection increases S phase initiation in the DZ. **a,** OVA-primed recipient mice received 5 x 10^6 B1-8^{hi} DEC$205^{+/+}$ and B1-8^{hi} DEC$205^{-/-}$ B cells at a 15:85 or 50:50 ratio. On day 6 after boosting with NP-OVA, mice that received the 15:85 transfer were injected with αDEC-OVA; mice that received the 50:50 transfer were injected with PBS. At 48 hours after treatment, draining lymph nodes were analyzed by flow cytometry. A representative plot showing EdU and BrdU incorporation among GC B cells is shown. **b,** Percent of early (E), mid/late (M/L), and post- (P) S phase GC B cells of B1-8^{hi} DEC$205^{+/+}$ (left) and B1-8^{hi} DEC$205^{-/-}$ (right) genotypes with a DZ surface phenotype. Black squares represent αDEC-OVA treatment; white squares represent PBS controls. Data represent two independent experiments with 6-7 mice per condition in total. Squares in **b** represent mean values; error bars = SEM.

The above findings suggest that selected GC B cells initiate additional cell cycles in the DZ before returning to the LZ. I reasoned that if selected B cells accrue more cell divisions in this manner, then they should spend more time in the DZ.

To test this idea, I used photoactivation to examine whether selected B cells that present higher levels of antigen dwell longer in the DZ. GCs were induced in OVA-primed mice that received B1-8^{hi} DEC205$^{+/+}$ B cells expressing a photoactivatable green fluorescent protein (B1-8^{hi} PAGFP^{+}) and B1-8^{hi} DEC205$^{-/-}$ B cells. On day 6 after the boost, selection was induced by injecting αDEC-OVA (Figure 2.10).

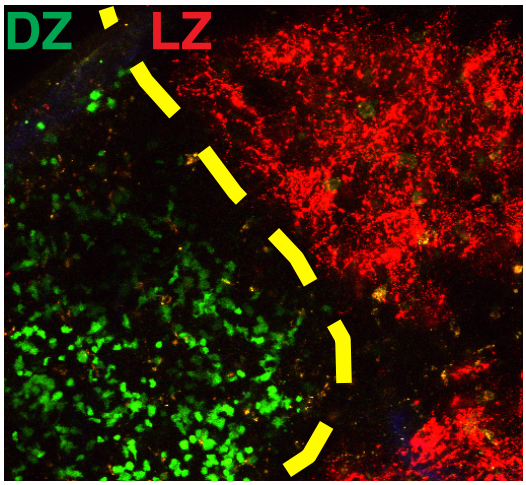

Figure 2.10. Photoactivation of GC B cells in the DZ of ongoing immune responses. OVA-primed mice received adoptive transfers of 5 x 10^{6} B1-8^{hi} PAGFP^{+} and B1-8^{hi} DEC205$^{-/-}$ B cells at a 15:85 ratio or 5 x 10^{6} B1-8^{hi} PAGFP^{+} B cells alone as a control. Recipient mice were then boosted with NP-OVA, and mice receiving the 15:85 mixed B cell transfer were injected with αDEC-OVA on day 6. On day 7, NP-tdTomato was injected to visualize the LZ (red). On day 8, DZ cells were photoactivated subjacent to the red fluorescently labeled LZ areas. GC B cells were then analyzed by flow cytometry at 0 or 6 hours after photoactivation.

After 48 hours, when selection is still ongoing, DZ cells were photoactivated and lymph node cells were then analyzed by flow cytometry either 0 or 6 hours after photoactivation (Figure 2.11).

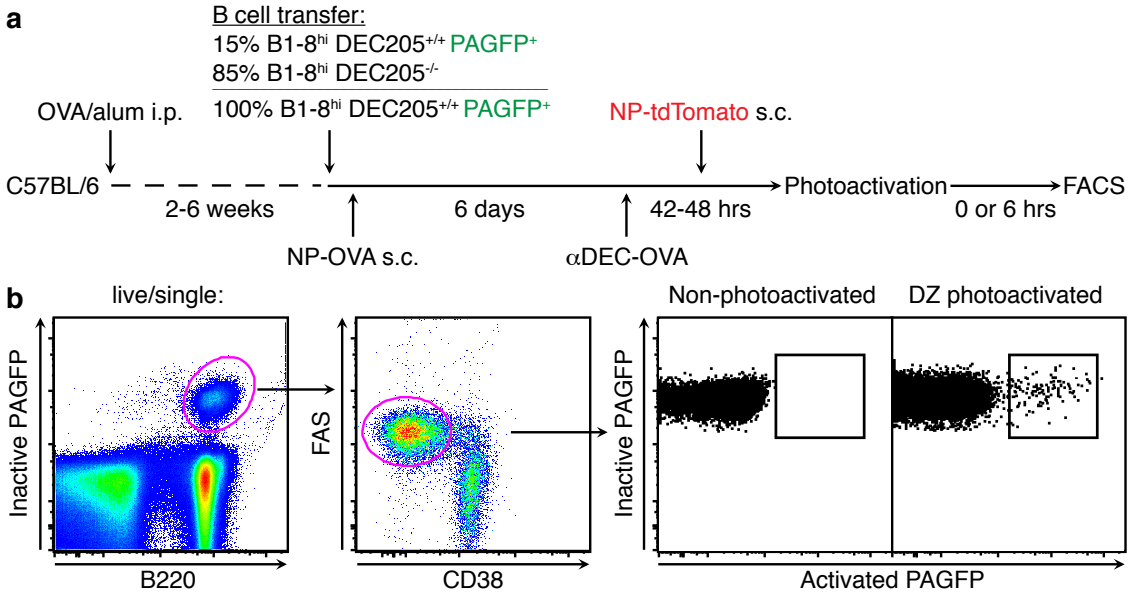

Figure 2.11. Experimental protocol for photoactivation of the DZ and flow cytometric analysis. a, Diagrammatic representation of experimental protocol used in Figure 2.10 and 2.12. **b,** Gating strategy used in flow cytometric analysis of DZ-photoactivated GC B cells. Cells of interest were gated as live/single, $B220^{+}PAGFP^{+}CD38^{-}FAS^{+}$Active $PAGFP^{+}$.

57% of photoactivated DZ cells became LZ cells after 6 hours under control conditions. In contrast, B1-8^{hi} $PAGFP^{+}$ cells in the midst of expansion became LZ cells at nearly half this rate (Figure 2.12). Thus, GC B cells undergoing selection due to increased antigen presentation reside longer in the DZ, providing them more time to divide before returning to the LZ. I conclude that T_{FH} cells regulate

the number of cell divisions initiated by a GC B cell that passes through the DZ, in direct proportion to the amount of antigen presented.

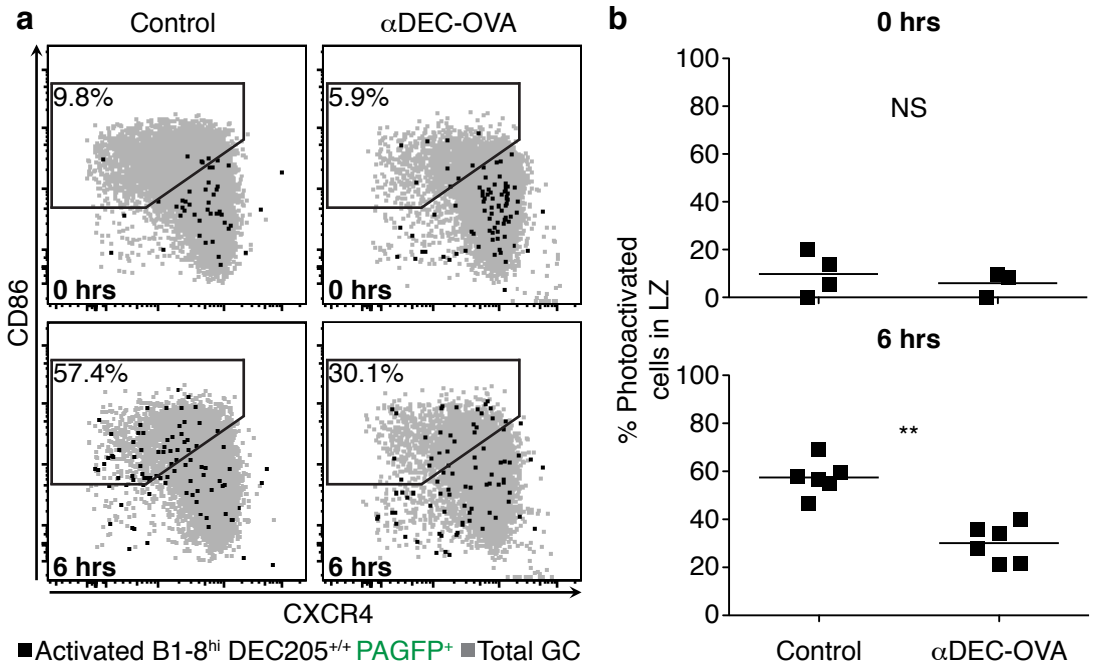

Figure 2.12. T cell-mediated selection in the GC involves longer DZ residence time. a, Representative flow cytometry plots are shown displaying CD86 and CXCR4 surface phenotype at 0 and 6 hours after photoactivation. Gates for LZ cells are shown ($CD86^{+}CXCR4^{low}$) among photoactivated GC B cells. **b,** Percent of photoactivated B1-8^{hi} $PAGFP^{+}$ GC B cells with a LZ surface phenotype at 0 or 6 hours after photoactivation. Each symbol represents one mouse. Data represent multiple independent experiments. ** p = 0.0022, two-tailed Mann-Whitney test.

2.4. Germinal center selection in the polyclonal immune response

I next sought to test if the variable number of DZ divisions that selected cells undergo might be reflected in the polyclonal system. To this end, I examined if BCR affinity in polyclonal GCs is correlated with increased cell division, using the well-characterized response of C57BL/6 mice to NP (Allen et al., 1988). To generate polyclonal GCs, I immunized non-Ig transgenic, tTA-H2B-mCh mice with NP-OVA. Beginning on day 12.5 after immunization, DOX was administered for 36 hours and mCh^{Hi} and mCh^{Lo} GC B cells, representing lesser and greater extents of proliferation, respectively, were isolated by cell sorting (Figure 2.13).

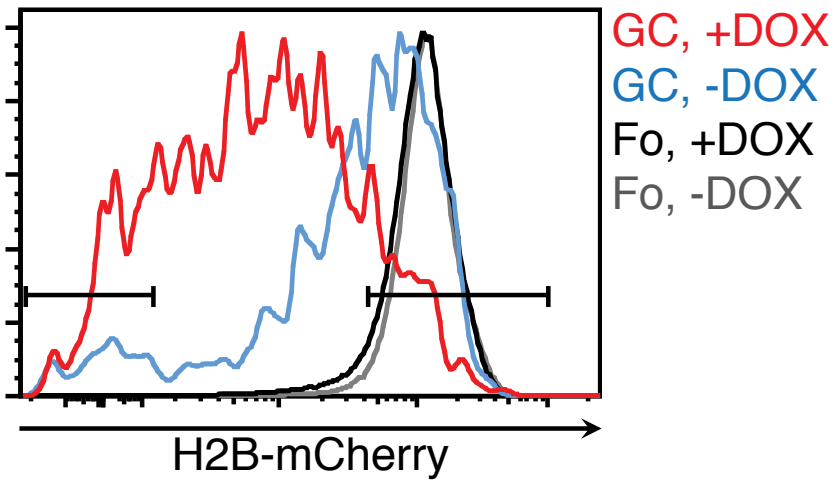

Figure 2.13. Use of the tTA-H2B-mCh system to analyze polyclonal GC B cells. tTA-H2B-mCh mice were immunized with NP-OVA in alum and administered DOX for 36 hours beginning at 12.5 days after immunization. Representative histogram is shown displaying H2B-mCh expression among GC B cells and mCh^{Hi} and mCh^{Lo} gates used for cell sorting and analyzing antibody gene mutations in Figures 2.14, 2.15, and 2.16.

Anti-NP GCs frequently utilize the V_H186.2 family of antibody genes, in which a tryptophan to leucine mutation at position 33 (W33L) increases antibody affinity by approximately tenfold. Among the mCh^{Lo} cells, I found that 35.9% were $W33L^+$; only 6% of mCh^{Hi} cells, which underwent fewer divisions, were $W33L^+$ (Figure 2.14, $p < 0.0001$).

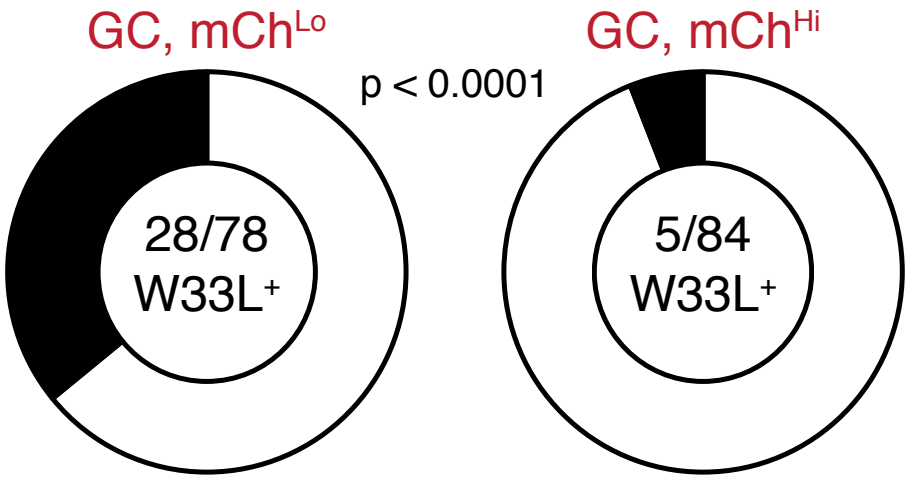

Figure 2.14. Affinity-enhancing mutations in polyclonal GCs are associated with increased cell division. V_H186.2 antibody genes from mCh^{Hi} (right) and mCh^{Lo} (left) GC B cells (using gates shown in Fig. 2.13) were cloned and sequenced on day 14 after NP-OVA immunization. The number of $W33L^+$ clones among total V_H186.2 sequences analyzed is shown in center of pie chart and was compared using Fisher's Exact test. Data are pooled from 2 independent experiments with 2 mice per experiment.

Thus, affinity-based selection in polyclonal GCs is associated with increased proliferation. Notably, mCh^{Lo} cells are not all $W33L^+$, and some $W33L^+$ mutants are found among mCh^{Hi} cells. This likely reflects the fact that the progeny of

proliferating high affinity mutants will accrue additional mutations that can affect BCR affinity either positively or negatively, leading these subclones to undergo different rates of proliferation, death or differentiation.

2.5. Regulation of somatic hypermutation in the germinal center

~1 somatic mutation per 10^3 base pairs is predicted to occur in the antibody gene during each cell cycle in the GC (McKean et al., 1984). Thus, because T_{FH} cells regulate the number of cell divisions in the GC, they might also regulate the amount of hypermutation that GC B cells accumulate. To examine this, I immunized tTA-H2B-mCh mice with NP-OVA, purified mCh^{Hi} and mCh^{Lo} GC B cells by cell sorting, and analyzed the J_H4 intron, since this non-coding region is hypermutated but not subjected to selection (Jolly et al., 1997). Indeed, GC B cells that proliferated more were significantly more mutated than GC cells that divided less (Figure 2.15, $p < 0.0001$).

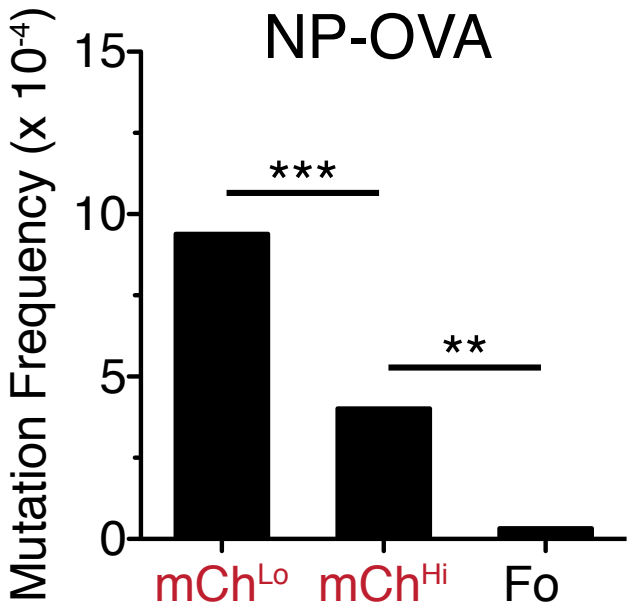

Figure 2.15. GC B cells that undergo more cell divisions accumulate a greater degree of somatic hypermutation. Mutation frequency within the J_H4 intron among mCh^{Hi} and mCh^{Lo} GC B cells and follicular (Fo) B cells is displayed. Cell sorting was performed on day 7 after NP-OVA immunization, following 36 hours on DOX. Data are pooled from 2 independent experiments with 2-3 mice per experiments and involve analysis of over 160 clones for GC B cells and 51 clones for follicular B cells. ** $p = 0.0033$; *** $p < 0.0001$, χ^2 test with Yates correction.

High levels of hypermutation are required to generate high affinity antibodies to HIV-1 that neutralize a broad diversity of viral variants, thus presenting a major obstacle to HIV-1 vaccine development (Scheid et al., 2009; Scheid et al., 2011; Walker et al., 2009; West et al., 2014a; Wu et al., 2010; Xiao et al., 2009). To determine if hypermutation accumulates differentially among GC B cells responding to HIV-1 gp120, tTA-H2B-mCh mice were immunized with $HIV\text{-}1_{YU2}$ gp120 and GC B cells were sorted based on mCh fluorescence. B cells in these

GCs that divided the most were also significantly more mutated than lesser divided mCh^{Hi} GC or follicular B cells (Figure 2.16).

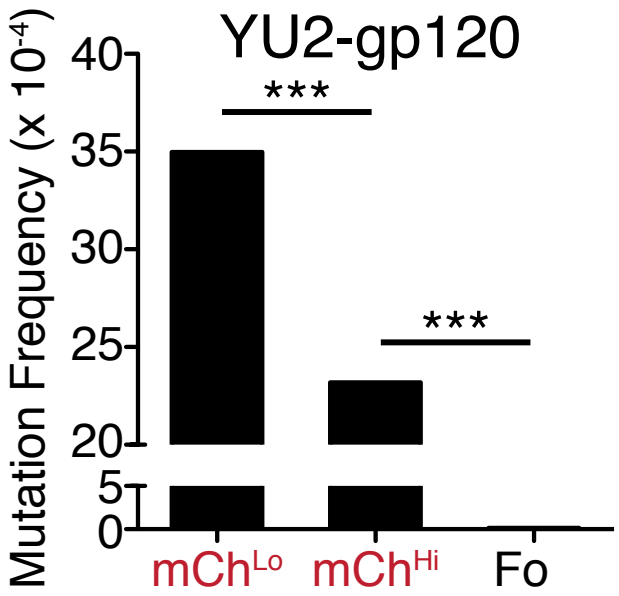

Figure 2.16. Somatic hypermutation is correlated with cell division in anti-gp120 GCs. Mutation frequency in the J_H4 intron was assessed in tTA-H2B-mCh mice on day 9 after immunization with YU2-gp120. Gates used for sorting mCh^{Hi} and mCh^{Lo} GC B cells are shown in Figure 2.13. Data are pooled from 2 independent experiments with 2-3 mice per experiment. Over 140 clones each were analyzed for mCh^{Hi} and mCh^{Lo} GC B cells and 94 clones were analyzed for follicular (Fo) B cells. *** $p < 0.0001$, χ^2 test with Yates correction.

Thus, T cells control the number of times that B cells divide in the DZ before migrating to the LZ, and increased cell division is associated with both higher BCR affinity and hypermutation (Gitlin et al., 2014).

Chapter 3:

T cell help controls the speed of the cell cycle in germinal center B cells

3.1. Transcription regulation during germinal center selection

Having found that T cell-mediated selection regulates the retention time of GC cells in the DZ, I sought to explore whether additional mechanisms might contribute to selection. To this end, I first sought to determine if GC B cells receiving enhanced T cell help display a specific change in transcriptional profile. However, αDEC-OVA-induced selection increases the fraction of cells in the S/G2/M phases of the cell cycle (Gitlin et al., 2014; Victora et al., 2010), potentially biasing the results of bulk gene expression analysis. Therefore, transcriptional profiles of control and selected DZ cells in the G1 phase of the cell cycle were compared. To isolate these cells, I bred DsRed and fluorescent ubiquitination-based cell cycle indicator ($Fucci^{tg}$) transgenic mice onto the $B1\text{-}8^{hi}$ $DEC205^{+/+}$ background described above (Aiba et al., 2010; Sakaue-Sawano et al., 2008). $B1\text{-}8^{hi}$ $DsRed^{+}$ $Fucci^{tg}$ DZ cells in the G1 phase could then be isolated by cell sorting based on fluorescence (Figure 3.1).

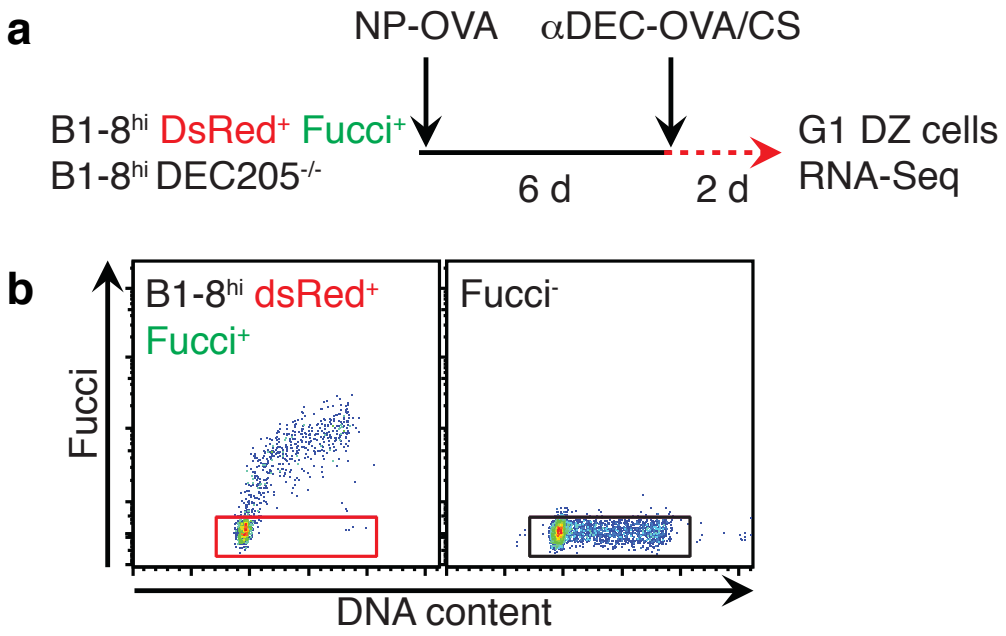

Figure 3.1. Experimental strategy to analyze gene expression in G1 DZ cells during T cell-mediated selection and control conditions. a, Experimental protocol used for transcriptional profiling data on G1 DZ cells. **b,** Flow cytometry plot showing fluorescent separation of G1 and S/G2/M cell cycle phases among B1-8^{hi} DsRed^{+} Fucci^{tg} GC B cells.

Comparing these cells by RNA sequencing after 48 hours of treatment with either αDEC-CS or αDEC-OVA revealed that, even when comparing the same cell cycle phase, T cell-mediated selection induced cell cycle and metabolic gene expression programs, including the metabolism of nucleotides (Figure 3.2).

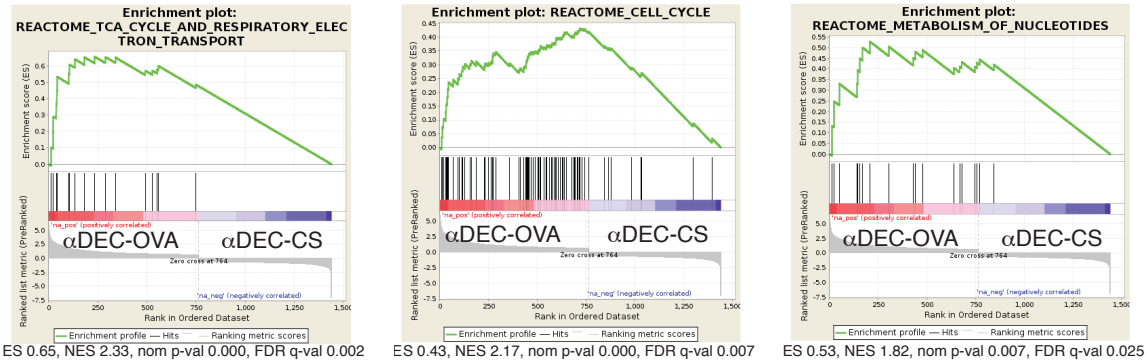

Figure 3.2. T cell help regulates cell cycle and metabolic gene expression programs in selected GC B cells. Enrichment plots are shown for selected gene sets from the Broad GSEA mSig database. Data are from experiment described in Figure 3.1 and corresponding text.

To analyze potential transcription factors whose activity might be induced by T cell help, we performed gene set enrichment analysis of transcription factor targets and found that T cell help regulated target genes downstream of c-Myc and the E2F family of transcription factors. This is consistent with previous work that found that T cell help directly induces expression of c-Myc in the LZ (Calado et al., 2012; Dominguez-Sola et al., 2012). Thus, target gene transactivation by c-Myc continues to be apparent as selected cells move to the DZ (Figure 3.3).

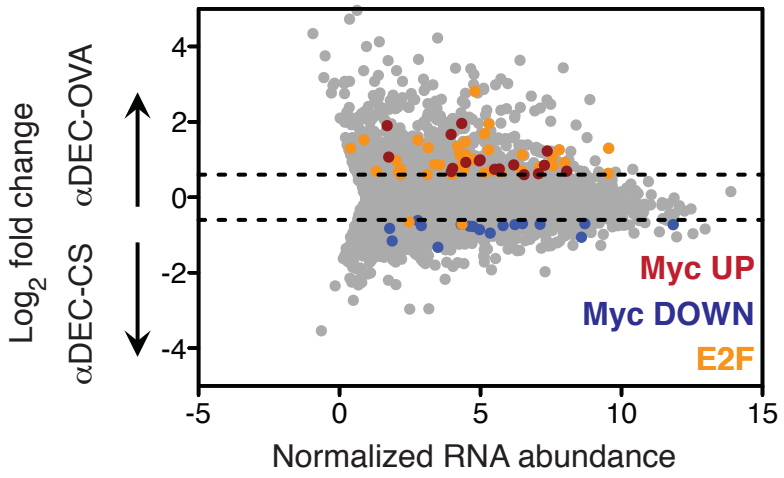

Figure 3.3. T cell help induces target genes downstream of c-Myc and E2F transcription factors. RNA sequencing analysis displaying genes up- or down-regulated by a fold-change of at least 0.6 (log2) after αDEC-OVA or αDEC-CS injection. For clarity, only regulated c-Myc and E2F target gene sets are shown. Normalized RNA abundance was calculated as [$\log_2$(αDEC-CS) + $\log_2$(αDEC-OVA)]/2. Results represent 2 independent experiments.

E2F transcription factors are the primary drivers of the cell cycle and are repressed by the retinoblastoma (Rb) protein. Cyclin-dependent protein kinases (CDKs) phosphorylate Rb, thereby relieving E2F of Rb-mediated repression (Chellappan et al., 1991; Chen et al., 2009). Consistent with our transcriptional data, increased T cell help led to enhanced Rb phosphorylation in selected GC B cells (Figure 3.4). E2F and c-Myc promote cell cycle phase transitions, regulate nucleotide metabolism, and control DNA replication dynamics (Bester et al., 2011; Chen et al., 2009; Dang, 2012; Dominguez-Sola and Gautier, 2014), suggesting that T cell-mediated selection might control the cell cycle dynamics of selected GC B cells.

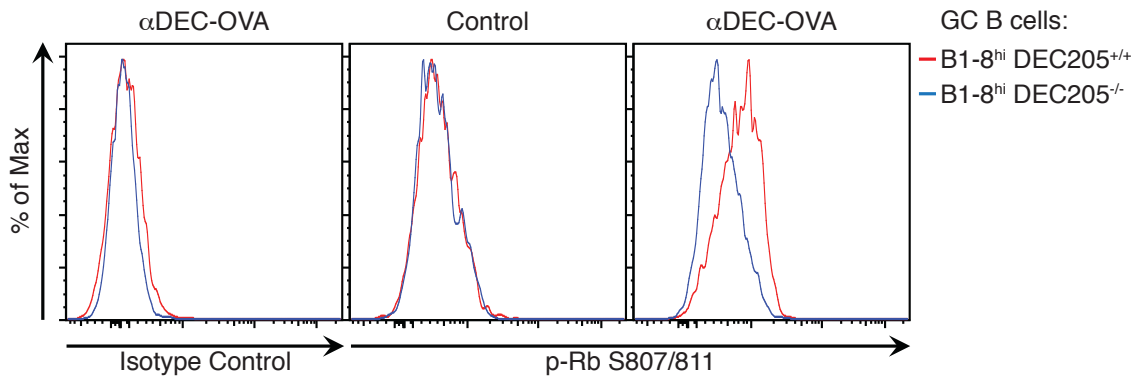

Figure 3.4. T cell help induces increased Rb phosphorylation in selected GC B cells. Histograms show intracellular Rb phosphorylation in B1-8^{hi} DEC205$^{+/+}$ and B1-8^{hi} DEC205$^{-/-}$ GC B cells on day 2 after treatment with αDEC-OVA or αDEC-CS (control). Results are representative of 3 independent experiments.

3.2. Regulation of cell cycle dynamics in the germinal center

To examine cell cycle dynamics during GC selection, we utilized the sequential EdU/BrdU double-pulse method developed above together with DNA content staining with 7-aminoactinomycin D (7-AAD) to determine current cell cycle stage. At 0.5 hours after the double-pulse, early S phase cells (EdU^{-}BrdU^{+} labeled) had replicated such a small fraction of their genome that their DNA content resembled that of G1 phase cells (Figure 3.5). Mid/late-S phase cells (EdU^{+}BrdU^{+} labeled) appeared to span the spectrum of S phase; post-S phase cells (EdU^{+}BrdU^{-} labeled) were either in G2/M phase or in G1 phase of the subsequent cell cycle.

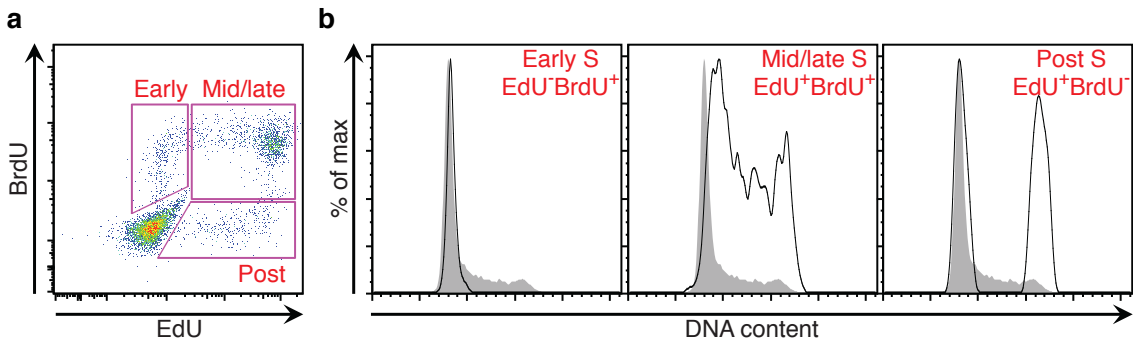

Figure 3.5. Combining sequential EdU/BrdU double-pulse method with DNA content staining. a, Representative pseudocolor plot displays B1-8^{hi} GC B cells from draining lymph nodes of mice that were injected intravenously with EdU followed 1 hour later by BrdU and then analyzed by flow cytomtery 0.5 hours later. **b,** DNA content plots show gated cell populations shown in **a** (black) against total GC B cell population (solid gray).

B1-8^{hi} DEC205$^{+/+}$ and B1-8^{hi} DEC205$^{-/-}$ post-S phase GC B cells were similarly distributed between G2/M and G1 under control conditions, indicating similar rates of progression through G2/M. By contrast, inducing selection by αDEC–OVA induced B1-8^{hi} DEC205$^{+/+}$ but not B1-8^{hi} DEC205$^{-/-}$ GC B cells to return to G1 more quickly, indicating rapid and selective G2/M progression (Figure 3.6). Thus, T cell-mediated selection accelerates progression through G2/M.

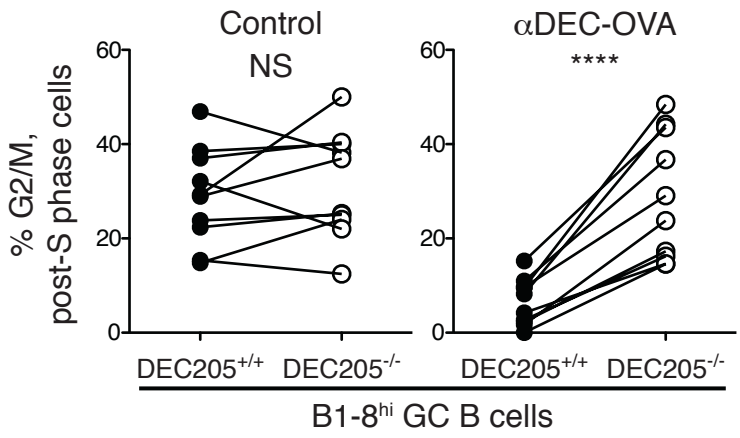

Figure 3.6. T cell help accelerates progression of selected GC B cells through G2/M phases. Mean percent of cells in G2/M among EdU^+BrdU^- (post-S phase) B1-8^{hi} $DEC205^{+/+}$ and B1-8^{hi} $DEC205^{-/-}$ GC B cells after treatment with αDEC-OVA or αDEC-CS (control) 2 days earlier. Lines connect indicated cell populations from the same animal. Data represent 2 independent experiments. **** $p < 0.0001$, two-tailed paired T test.

To examine S phase dynamics during T cell-mediated selection, GC B cells were followed at 2.5 and 5 hours after a sequential EdU/BrdU double-pulse. At 2.5 hours, cells which were in early S phase at 0.5 hours (EdU^-BrdU^+ labeled) had by this time progressed into mid/late-S phase as determined by DNA content. Moreover, with only these 2 additional hours, selected GC B cells accumulated more DNA content than non-selected GC B cells, indicating that they had replicated their genomes more rapidly than control cells (Figure 3.7). After 5 hours, nearly half of the EdU^-BrdU^+ cells had completed S phase, reaching G2/M or the following G1. T cell help induced by aDEC-OVA significantly accelerated progression of B1-8^{hi} $DEC205^{+/+}$ GC B cells through S phase because a far

greater fraction of these cells completed DNA replication within 5 hours than non-selected B1-8^{hi} DEC205$^{-/-}$ GC cells (Figure 3.8). Thus, T cell help accelerates progression through both the S and G2/M phases of the cell cycle.

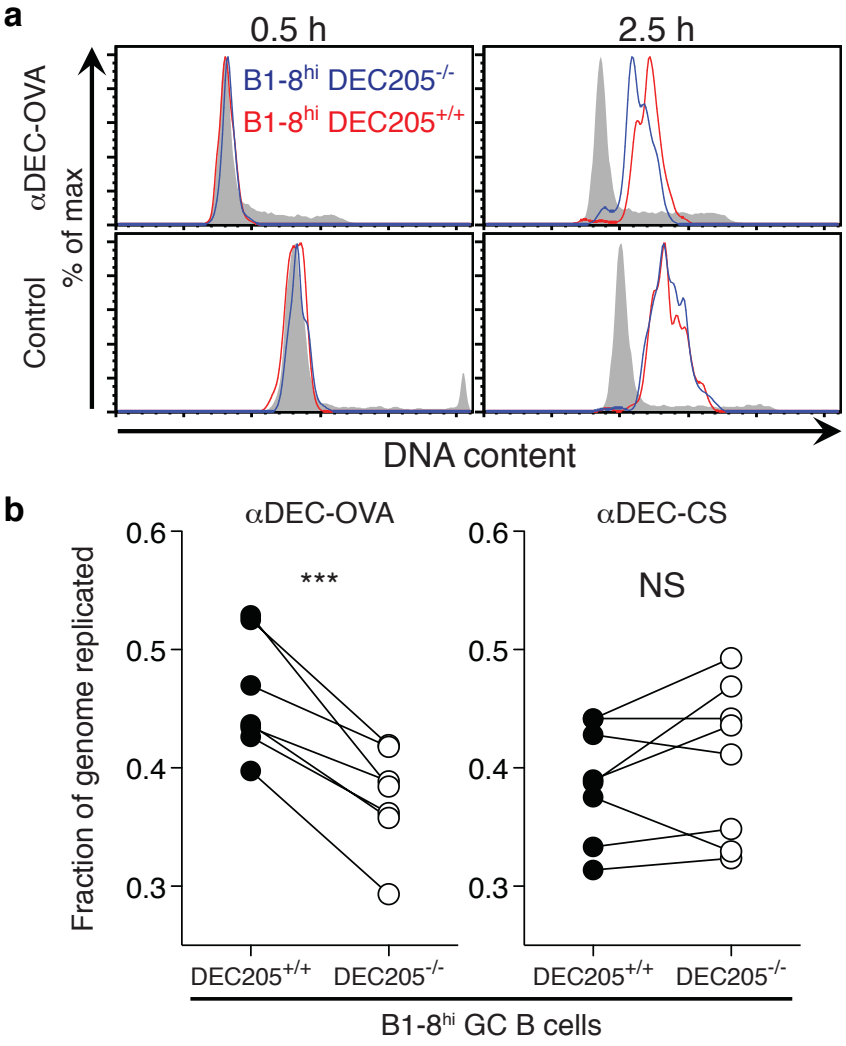

Figure 3.7. T cell help accelerates the speed of DNA replication. a, Histograms show DNA content accumulation among EdU^{-}BrdU^{+} GC B cells at 0.5 and 2.5 hours after the EdU/BrdU double-pulse. Solid gray represents all GC B cells within the same animals. **b,** Median fluorescence intensity (MFI) was measured in EdU^{-}BrdU^{+} GC B cells 2.5 hours after the EdU/BrdU double-pulse. Fraction of the genome was then calculated as [(MFI of EdU^{-}BrdU^{+} GC cells)/(MFI of G1 phase cells)]-1. *** p = 0.0007, paired T-test.

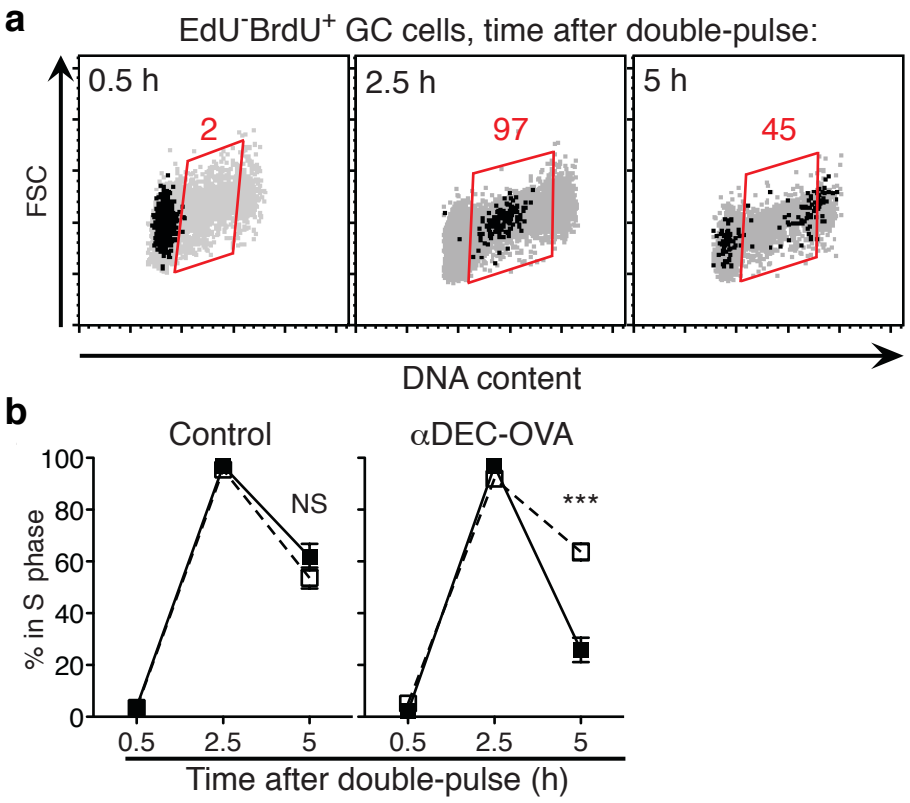

Figure 3.8. T cell help accelerates progression of selected GC B cells through S phase. a, Representative flow cytometry plots show progression of $EdU^{-}BrdU^{+}$ GC B cells (black dots) through the cell cycle phases at 0.5, 2.5, and 5 hours after an EdU/BrdU double-pulse. **b,** Mean percent of GC B cells in S phase gate shown in **a** among $EdU^{-}BrdU^{+}$ B1-8^{hi} $DEC205^{+/+}$ (black squares) and B1-8^{hi} $DEC205^{-/-}$ (white squares) cells.

I next sought to validate these findings in the context of the polyclonal immune response. To do so, I utilized the antibody response to NP in C57BL/6 mice. As described above, high affinity clones in anti-NP GCs carry the W33L mutation, and additionally a lysine to arginine mutation at position 59 (K59R) in the V_H186.2 antibody gene (Allen et al., 1988; Furukawa et al., 1999). Mice immunized with

NP-OVA 2 weeks earlier were pulsed with EdU, followed by BrdU to inhibit further EdU uptake after 30 minutes (Figure 3.9).

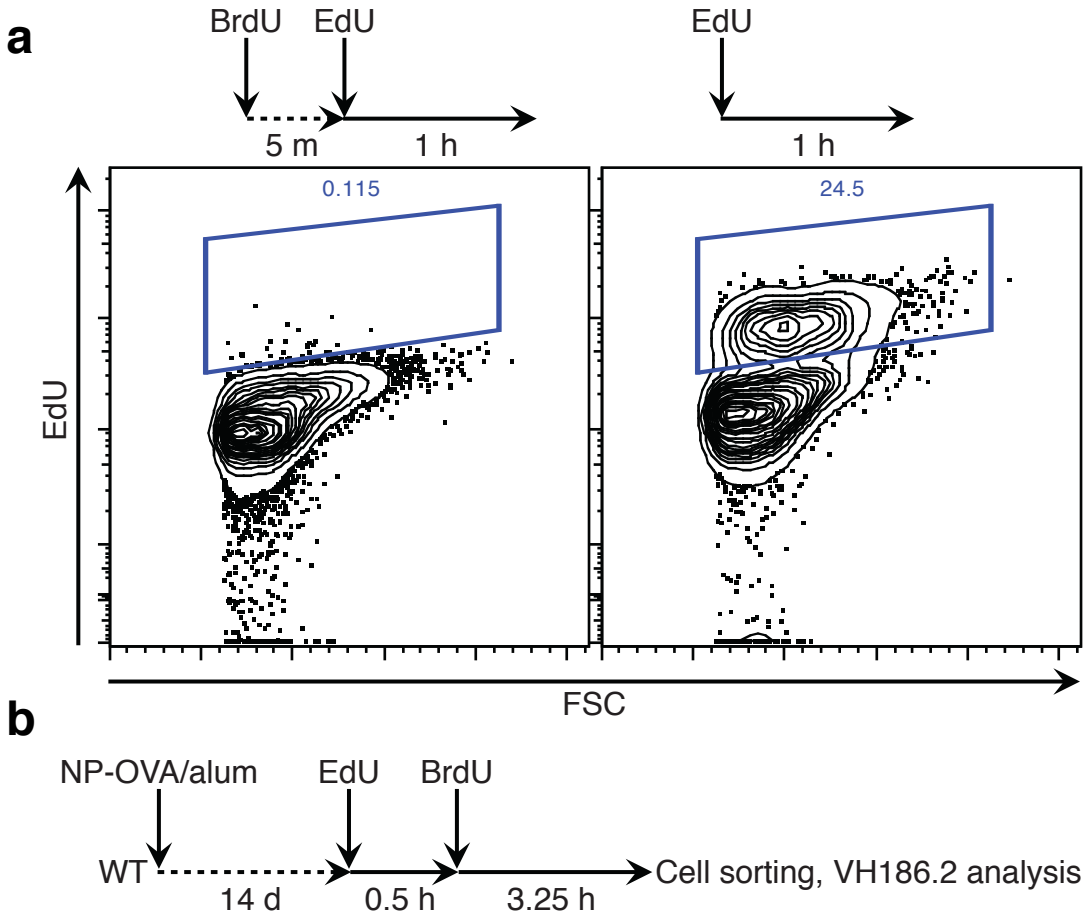

Figure 3.9. EdU/BrdU labeling of polyclonal GCs. a, C57BL/6 mice were injected with EdU only (right) or with BrdU 5 minutes prior to EdU (left). Flow cytometry of GC B cells in peyer's patches shows that the presence of BrdU inhibits EdU uptake. **b,** Experimental protocol used in Figure 3.10. C56BL/6 mice were immunized intraperitoneally with NP-OVA in alum. On day 14, mice were injected with EdU and then 0.5 hours later with BrdU. After 3.25 hours, cells were sorted using the gates shown in Figure 3.10 and antibody gene sequences were analyzed for affinity-enhancing mutations.

After 3.25 hours, two populations of EdU^+ GC cells are evident based on DNA content: (1) EdU^+ S/G2/M cells, which consist of cells that were in early S phase during the EdU injection and/or cells that progressed slowly through S/G2/M; (2) EdU^+ G1 cells, which consist of cells that were near completion of S phase during the EdU injection and/or progressed rapidly through S/G2/M (Figure 3.10A). Thus, if rapid progression through S/G2/M is also feature of polyclonal immune responses, then affinity-enhancing mutations should be enriched in the EdU^+ G1 population. Cloning and sequencing of the antibody variable regions revealed that EdU^+ G1 cells were indeed significantly enriched in high affinity clones compared to EdU^+ S/G2/M cells (Figure 3.10B). Thus, affinity-enhancing mutations are associated with rapid S/G2/M progression during the polyclonal B cell response.

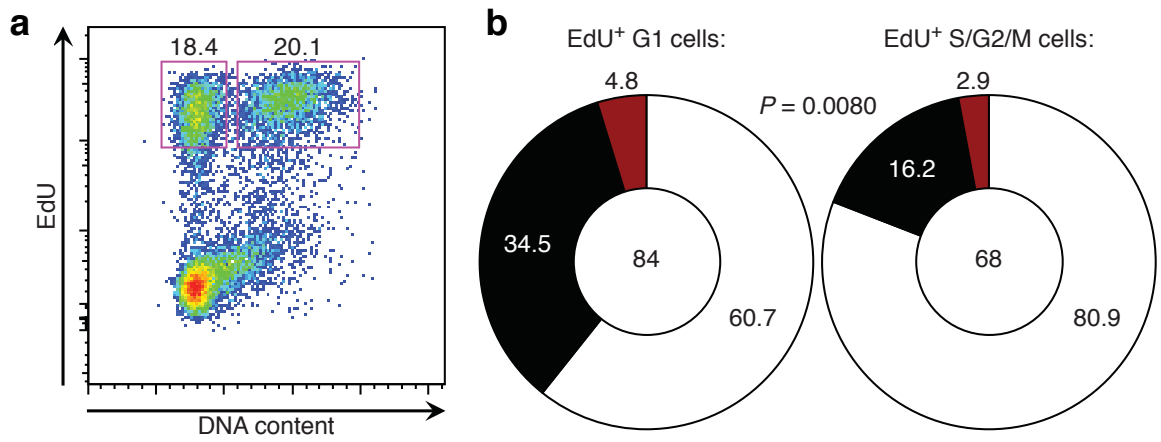

Figure 3.10. Affinity-enhancing mutations are associated with rapid progression through S/G2/M in polyconal GC responses. a, C57BL/6 mice were treated as described in Figure 3.09B and corresponding text. A representative pseudocolor plot is shown with gates used to sort GC B cells that are EdU^+ and in either the G1 or S/G2/M cell cycle phases based on DNA content. **b,** Pie charts show the frequency of W33L (black) and K59R (red) affinity-enhancing mutations among V_H186.2 sequences analyzed in sorted EdU^+ G1 or EdU^+ S/G2/M GC B cells. One sequence was positive for both W33L and K59R mutations and is counted in the black slice of EdU^+ S/G2/M cells. The number of clones analyzed is displayed in the center of the pie charts. Statistical significance was assessed with the Fisher's exact test. Results are pooled from 2 independent experiments with 10 mice each.

3.3 Mechanism of DNA replication control in the germinal center

Upon committing to the cell cycle, GC B cells spend most of their time in S phase until completion of the cell cycle (Gitlin et al., 2014). I therefore sought to understand the basis for T cell-mediated regulation of S phase progression. It has long been understood that S phase length is developmentally controlled

(Nordman and Orr-Weaver, 2012). For example, the earliest embryonic cell cycles involve rapid S phases. Following the midblastula transition, embryonic S phases lengthen considerably. In this context, regulation of S phase is controlled at the level of DNA replication initiation (Blumenthal et al., 1974; Collart et al., 2013; Hyrien et al., 1995; McKnight and Miller, 1977). Namely, early S phases are rapidly completed due to an increased number of replication origins that fire with a high level of synchronicity. As development proceeds, fewer replication origins fire and do so much less synchronously, causing certain genomic regions to be replicated relatively later in S phase than others due to a relative paucity of origins in late-replicating regions.

Based on these findings, I first sought to evaluate the dynamics of DNA replication initiation. For this purpose, I sorted and sequenced the genomes of B1-8^{hi} DEC205$^{+/+}$ GC B cells in G1 and S phase after treatment with αDEC-CS or after inducing their selection with αDEC-OVA. In a sorted population of S phase cells, regions of the genome that replicate early during S phase, and which thus contain a higher density of origins, have higher copy number than regions that replicate later during S phase. Normalizing the read depth of S phase cells to a matched sample of G1 phase cells corrects for any sequence elements that might bias read depth (Koren et al., 2014; Koren et al., 2012). Using this method, we obtained global profiles of the temporal order of DNA replication. Independent profiles generated in this manner were highly correlated with each other ($r > 0.91$)

and displayed significant similarity (r > 0.73) to replication timing profiles of mouse lymphocytic leukemia cells (Figure 3.11) (Yaffe et al., 2010).

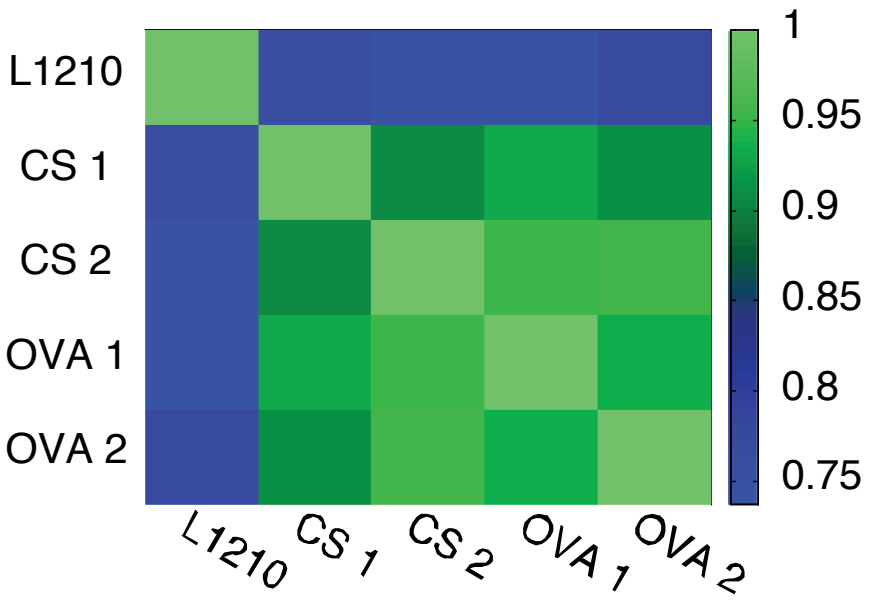

Figure 3.11. Correlation in replication timing profiles between biological conditions, biological replicates, and the L1210 mouse lymphocytic leukemia cell line. Correlation matrix shows degree of similarity in the indicated replication timing profiles.

Surprisingly, DNA replication initiation dynamics among selected and non-selected GC B cells was essentially identical (r = 0.98), involving the same locations and activation times of replication origins throughout the genome (Figure 3.12). Thus, T cell help induces a proportional condensing of the replication timing program during S phase, preserving the overall dynamics of replication initiation on a shorter timescale.

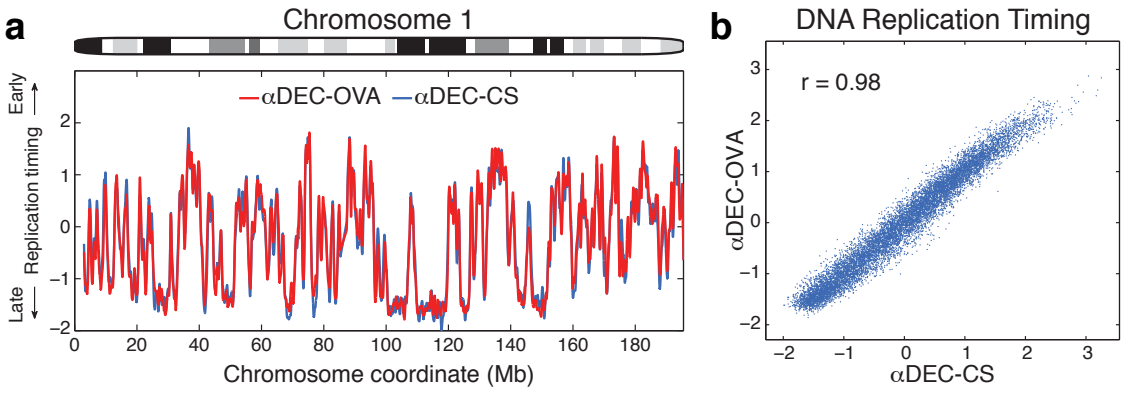

Figure 3.12. T cell-mediated acceleration of S phase does not involve altering the initiation dynamics of DNA replication. a, DNA replication timing for chromosome 1 is shown. Replication timing values were determined by analyzing the ratio of DNA copy number between S and G1 phase B1-8^{hi} DEC205$^{+/+}$ GC B cells treated with either αDEC-CS or αDEC-OVA. **b,** Genome-wide correlation plot of replication timing in αDEC-CS and αDEC-OVA conditions.

In vitro, DNA replication forks can be accelerated by enhanced c-myc, CDK activity and nucleotide metabolism (Anglana et al., 2003; Bester et al., 2011; Malinsky et al., 2001), but a physiological role for S phase regulation by these means has not been observed. Because T cell-mediated selection elicits similar changes in GC B cells, I sought to visualize the progression of DNA replication forks by single-molecule analyses (Jackson and Pombo, 1998). In order to do so, mice were administered the nucleoside analog 5-iodo- 2'deoxyuridine (IdU) for 20 minutes following αDEC-OVA or control treatment (Figure 3.13).

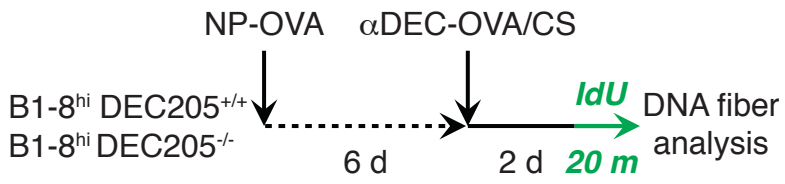

Figure 3.13. Single-molecule imaging of DNA replication in GC B cells. Experimental protocol used in Figure 3.14. OVA-primed recipient mice received an adoptive transfer of B1-8^{hi} DEC205$^{+/+}$ and B1-8^{hi} DEC205$^{-/-}$ B cells at a 15:85 or 50:50 ratio and were then subcutaneously boosted with NP-OVA. On day 6 after the boost, mice receiving the 15:85 transfer were treated with αDEC-OVA, and mice receiving the 50:50 transfer were treated with αDEC-CS. After 2 days, mice were pulsed with IdU for 20 minutes before cell sorting and processing for imaging analyses.

B1-8^{hi} DEC205$^{+/+}$ GC B cells were isolated by cell sorting and DNA fibers were stretched on glass slides to measure the lengths of replication tracks among individual DNA molecules. T cell-mediated selection significantly increased both the average length of replication tracks and the distribution of lengths of replication tracks (Figure 3.14, $p < 0.0001$). I conclude that T cell help accelerates S phase by increasing the speed of individual DNA replication forks, rather than by increasing the synchronicity or number of replication origins that are activated.

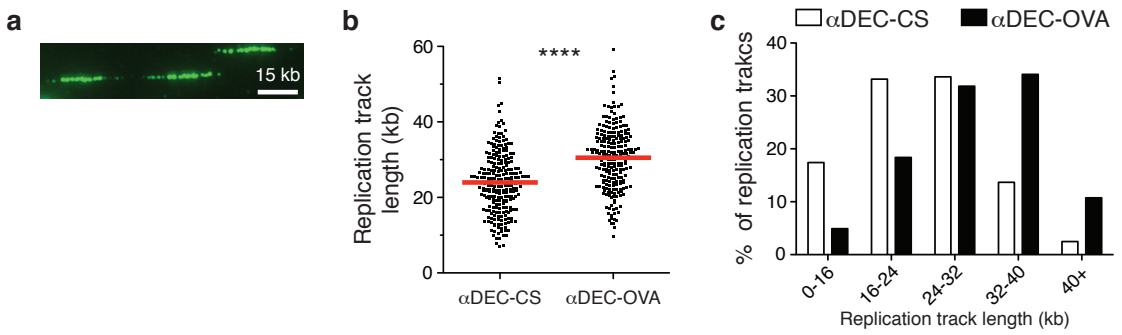

Figure 3.14. T cell help accelerates S phase by increasing the speed of DNA replication forks. a, Experiment was performed as described in Figure 3.13 and corresponding text. Representative IdU-labeled DNA fibers are shown. **b,** Dot plot displaying replication track lengths from B1-8^{hi} DEC205$^{+/+}$ GC B cells treated with αDEC-CS or αDEC-OVA. Each dot represents a measured fiber; red lines represent mean values. Results are pooled from 2 independent experiments involving over 220 measured fibers in total for each condition. **c,** Distribution of replication track lengths. *** $p < 0.0001$, two-tailed Mann-Whitney test.

Chapter 4:

Discussion

In 1884, Walther Flemming provided the first description of the germinal center as a site of intensely proliferating lymphocytes within secondary lymphoid organs (reviewed in Nieuwenhuis and Opstelten, 1984). Although Flemming proposed that the GC was as a source of lymphocytes, it is now well understood that the GC is, in fact, the site where affinity maturation takes place.

Affinity maturation refers to the serological phenomenon whereby antibody affinity rises gradually after infection or immunization (Eisen and Siskind, 1964). The GC accomplishes this task by clonal expansion of antigen-specific B cells, random SHM of their antibody genes, and subsequent selection of only those mutant antibody clones with increased affinity (Berek et al., 1991; Brown et al., 1992; Jacob et al., 1991b; Kocks and Rajewsky, 1988; McKean et al., 1984). Selected GC B cells differentiate into long-lived plasma cells, which predominantly populate the bone marrow and secrete high affinity antibodies, and memory B cells, which recirculate and can be activated upon encountering antigen to produce a robust secondary response (Smith et al., 1997; Tarlinton and Good-Jacobson, 2013). Thus, although affinity-based selection in the GC has a central role in the formation of humoral immunity, its dynamic basis has

been enigmatic. In this thesis, I have examined the underlying mechanisms and dynamics that allow B cells with the highest affinity for antigen to be selectively expanded in the GC.

4.1 Germinal center dynamics and selection

Early studies on the GC found that it could be divided into two microanatomical regions: a light zone (LZ) and a dark zone (DZ) (Nieuwenhuis and Opstelten, 1984). Histologically, these zones differed dramatically. The DZ contained larger cells undergoing mitosis (referred to as centroblasts); the LZ contained smaller, non-proliferative cells (referred to as centrocytes), as well as follicular dendritic cells (FDCs) and helper T cells. FDCs in the LZ were found to retain and display the inducing antigen for long periods of time in the form of immune complexes (Mandel et al., 1980; Mandel et al., 1981). These observations suggested that migration of B cells between the two zones must occur in order for B cells that diversify their receptors in the DZ to undergo antigen-driven selection in the LZ. Evidence for such migration was first provided by nucleotide-labeling studies that observed such exchange (Hanna, 1964). However, intravital imaging found that while B cells did migrate interzonally, cells in both zones were highly dynamic, morphologically similar, and could in fact synthesize DNA in both zones (Allen et al., 2007b; Hauser et al., 2007; Schwickert et al., 2007).

Combining photoactivation with intravital imaging helped reconcile these findings with the classical model of GC selection (Victora et al., 2010). Namely, GC B cells did indeed migrate interzonally, but with a net vector of movement from DZ to LZ, suggesting that only a limited number of selected LZ cells could return to the DZ to expand. These findings thereby provided confirmatory in vivo evidence for the cyclic re-entry model of selection (Kepler and Perelson, 1993; Oprea and Perelson, 1997). Moreover, while DNA synthesis took place in both zones, the completion of the cell cycle – G2/M – occurred predominantly in the DZ. Thus, LZ cells in the G1 phase might receive a signal to initiate S phase, but would then likely migrate to the DZ in order to finish S phase and proceed through the G2/M phases. Once in the DZ, B cells could then continue to initiate additional cell cycles before undergoing another round of selection in the LZ.

With these insights into GC dynamics, the mechanistic nature of the selecting agent in the LZ still remained unresolved. The main challenge in this regard was the dual nature of the BCR, as it can mediate both signal transduction and endocytosis of antigen for presentation to T cells. This issue was overcome by generating mixed GCs, composed mainly of DEC205$^{-/-}$ B cells mixed with a minor fraction of DEC205$^{+/+}$ B cells, with both subsets carrying the same B1-8^{hi} BCR specific for NP (Victora et al., 2010). Acute delivery of αDEC205 fused at its C-terminus to the carrier protein OVA, but not to an irrelevant protein antigen, induced the selective expansion of B1-8^{hi} DEC205$^{+/+}$ GC B cells by enhancing

their receipt of cognate T cell help. Importantly, the DEC205 antigen-delivery system was the first to separate the downstream functions of the BCR – it increased antigen presentation without engaging or cross-linking the BCR. This demonstrated that increasing pMHCII on the surface of a subset of GC B cells sufficed to induce their selection. Furthermore, differential antigen presentation in the GC was shown to be required for affinity maturation, since indiscriminately increasing pMHCII on all of the B cells in the GC through DEC205, thereby "blinding" GC B cells to the amount of antigen their BCRs can internalize, prevented both the selection of high affinity GC mutants and the maturation of serum antibody affinity. Thus, T cell help, rather than BCR cross-linking and/or signaling, is both a necessary and sufficient factor in GC selection.

4.2 T cell-mediated germinal center selection

The key question arising from the above studies, and which I have addressed in this thesis, is how T cell help regulates the dynamics of GC B cells in order to mediate the selective expansion of high affinity cells. In principle, reducing cell death and/or increasing proliferation could allow T cell help to produce selective expansion of a subset of high affinity cells in the GC. Notably, studies in which GC B cells were isolated from human tonsils found that these cells rapidly underwent apoptosis when cultured (Liu et al., 1989). Non-GC B cells isolated from the same tissue did not undergo apoptosis at such high rates. However,

stimulating tonsillar GC B cells in culture through their BCRs and by agonistic CD40 antibodies substantially prevented their death in vitro. These findings led to the notion that GC B cells are physiologically programmed to die by apoptosis unless rescued by such signals – a potential mechanism for antigen-driven selection, since high affinity cells would presumably receive such survival signals to either a greater extent or with greater likelihood than would lower affinity cells. In contrast, regulation of cell division in the GC, and whether it might play a role in affinity-based selection, had been far less studied and understood.

4.2.1. T cell-regulated proliferation dynamics in the germinal center

To gain insight into the dynamics of proliferation in the GC, I first sought to develop a tool that could measure the number of cell cycles a GC B cell has undergone. Conventional methods that are commonly used for this purpose include, among other techniques, CFSE dilution and nucleotide labeling. However, in the context of the GC, nucleotide labeling cannot provide dynamic information, and CFSE cannot be utilized due to the large number of cell divisions that B cells undergo at the T/B border, prior to GC coalescence.

The need for improved cell division techniques in vivo has been addressed in the developmental and stem cell biology fields through the use of “Tet-off” systems (Tumbar et al., 2004). These systems employ histone H2B proteins fused to

fluorescent proteins as markers of division, which in the case of this thesis was an H2B-mCherry protein. Thus, under steady state conditions, a tetracycline transactivator protein (tTA) drives expression of high levels of H2B-mCherry (Egli et al., 2007; Wiesner et al., 2005). When DOX is administered, tTA is repressed and can no longer induce further H2B-mCherry synthesis. Due to the extremely long natural half-lives of histone proteins (Foudi et al., 2009), H2B-mCherry levels will nevertheless be highly stable within cells that do not divide. However, cell division during DOX treatment will dilute H2B-mCherry in half, generating a division history among progeny cells that can be quantified based on the dilution of mCherry fluorescence intensities. By combining the tTA-H2B-mCh system with the DEC205 antigen-delivery system described above, I was able to demonstrate that GC B cells receiving increased T cell help undergo a greater number of cell cycles (Gitlin et al., 2014). The tTA-H2B-mCh system, and others like it, should prove generally useful to the field of immunology, since it allows cell division history to be followed without the need to adoptively transfer CFSE-labeled cells and with great experimental flexibility.

4.2.2. T cell-regulated dynamics of interzonal migration

How might selected GC B cells accrue more cell divisions than their competitors? To answer this question, we considered two potential models. First, selected GC B cells might be migrating more frequently between LZ and DZ. Thus, in a given

timeframe, selected GC B cells would pass more frequently through the DZ, where they would divide, and thus these cells would be able to accrue a greater number of cell divisions in total. Alternatively, during each visit to the DZ, selected GC B cells might dwell for a longer period of time, providing these cells with proportionally more time to undergo additional divisions. In this second model, non-selected competitors in the GC would spend less time in the DZ and thus a greater fraction of their time would be spent in the LZ, where they would be competing for T cell help rather than using their time to actively divide. These two models predict different dynamic behaviors in the DZ: the first model predicts that selected cells spend equal or less time in the DZ than non-selected cells; the second model predicts that selected cells would spend more time in the DZ than would non-selected GC B cells.

I therefore turned to photoactivation to determine how T cell help influences the residence time of selected cells in the DZ (Patterson and Lippincott-Schwartz, 2002; Victora et al., 2010). Using a photoactivatable GFP transgene in combination with the DEC205 antigen-delivery system, I found that GC B cells that received increased T cell help spent a longer period of time in the DZ. This finding indicated that the additional time that selected cells are allowed to spend in the DZ enables them to initiate a greater number of cell divisions before traveling back to the LZ to undergo another round of competition for T cell help. If more cell cycles are indeed initiated during each passage through the DZ, then a

greater fraction of cells entering S phase should be found within the DZ during selection. To this end, we developed a sequential nucleotide-pulsing strategy using EdU and BrdU that confirmed this prediction.

Taken together, these experiments indicate that the number of cell divisions per excursion to the DZ is variable, ranging from 1 to 6, and is regulated by the magnitude of T cell help. High affinity mutants that emerge in the GC are able to capture more antigen in the LZ, thereby allowing these cells to present more pMHCII to T cells. The help received by selected B cells then induces them to return to the DZ, where they subsequently reside for a longer period of time than their non-selected competitors. Non-selected cells in the GC are thus outcompeted over time, since they spend a lesser portion of their time in the DZ and are thereby able to proliferate fewer times overall.

Previous work using CXCR4-deficient GC B cells, which are restricted in their location to the LZ, found that these cells can nevertheless attain a DZ-like state, characterized by a surface phenotype reminiscent of DZ cells and the ability to proliferate and hypermutate (Bannard et al., 2013). This indicates that the DZ state does not require physical access to signals present in the DZ microenvironment. A “cellular timer program” was therefore proposed to explain these findings. In this model, a signal in the LZ that triggers the cell to become a DZ cell initiates a timer within the newly induced DZ cell. Upon completion of this

timer, the DZ cell would return to its LZ state. Of note, T cell help was considered a key candidate signal that could initiate such a timer. This model is consistent with the work described in this thesis, namely that T cell help initiates a DZ cellular timer and, moreover, that the magnitude of help received by the B cell might in fact determine the length of the DZ timer.

4.2.3. A selection-hypermutation positive feedback loop

To verify these findings in the polyclonal system, non-immunoglobulin transgenic mice bearing the tTA-H2B-mCh transgenes were utilized. Sorting GC B cells from tTA-H2B-mCh mice that had undergone greater or lesser amounts of proliferation revealed that affinity-enhancing mutations in polyclonal GCs are associated with more cell divisions. Moreover, as predicted by the idea that AID targets the antibody gene once per cell cycle (Deenick et al., 1999; Hasbold et al., 1998; Hodgkin et al., 1996; McCall and Hodgkin, 1999; McKean et al., 1984; Reina-San-Martin et al., 2003), highly divided GC B cells were subjected to a greater degree of somatic mutation. A positive feedback loop of selection-hypermutation therefore exists in the GC, whereby high affinity cells are instructed by T cell help to divide more than their competitors, and, in so doing, selected cells accumulate greater diversity through more frequent opportunities for hypermutation.

The positive feedback loop between selection and SHM has implications for understanding the development of effective antibody responses to certain pathogens, such as HIV-1. Broadly neutralizing antibodies to HIV-1 (bNAbs) exhibit an extraordinary degree of hypermutation and selection, which are required for the capacity of these antibodies to potently neutralize extremely diverse variants of HIV-1. For example, while most affinity-matured antibodies in humans carry 15-20 mutations, bNAbs carry 40-110 mutations (Scheid et al., 2009; Scheid et al., 2011; Tiller et al., 2007; Walker et al., 2009; West et al., 2014b; Xiao et al., 2009; Zhou et al., 2010). Notably, hypermutation of bNAbs extends even into the framework regions (FWRs) of the variable region (Klein et al., 2013), which provide structural support to the complementarity determining regions (CDRs) that typically mediate direct antigen binding (Amit et al., 1986; Amzel and Poljak, 1979).

In most cases, FWR mutations are selected against due to the high likelihood that such mutations will be deleterious to the overall structure of the antibody molecule (Wagner et al., 1995). Furthermore, classic experiments demonstrated that grafting CDRs from one antibody onto the FWRs of another antibody still maintain the specificity of the antibody from which the CDRs were derived (Jones et al., 1986). Yet in the context of bNAbs, mutations in FWR and CDRs have become crucial and interdependent, and reversion of FWR mutations in bNAbs

causes them to lose their potency and breadth (Klein et al., 2013). How such high levels of FWR mutations might be generated is therefore of great interest.

Our findings suggest a potential mechanistic basis for the development of bNAbs with these features. For example, during the development of bNAbs in the GC, mutant clones that represent stepwise intermediates, along the path to bNAb development, would be iteratively selected by T cell help. During these selection events, bNAb precursor cells would be induced to return to the DZ and reside there for an extended period of time, providing these cells with more time to undergo multiple rounds of cell division and hypermutation. Importantly, this would allow selected bNAb precursors to incur a serious of somatic mutations without being interrupted by an intervening round of selection in the LZ. Over time, these events might allow interdependent, affinity-enhancing mutations in the FWRs and CDRs to develop. By contrast, if every excursion to the DZ involved only a single cell division and somatic mutation before subjecting the mutant cell to selection in the LZ, then it would be far more difficult to develop FWR mutations. Nevertheless, these bursts of diversification in the DZ might only rarely occur, potentially explaining why a small fraction of infected patients develop bNAbs, and, even then, why these patients require several years to develop such antibodies.

4.3. Cell cycle regulation in the germinal center

I next sought to examine the molecular basis for T cell-mediated regulation of GC B cell dynamics in the DZ. To this end, I hypothesized that a concerted and specific change in gene expression would be evident among selected GC B cells in the DZ. However, providing GC B cells with more T cell help through αDEC205-OVA shifts a greater fraction of this population into the S/G2/M cell cycle phases (Gitlin et al., 2014; Victora et al., 2010). Thus, to control for this effect, a Fucci transgene was used to allow fluorescence-based cell sorting of G1 phase cells followed by genome-wide RNA sequencing of this population (Aiba et al., 2010; Sakaue-Sawano et al., 2008). Surprisingly, even when controlling for cell cycle phase in this manner, selected DZ cells in G1 nevertheless displayed significantly enhanced cell cycle and metabolic gene expression programs. Moreover, when GSEA for transcription factor target genes was performed, we found that targets downstream of the E2F family of transcription factors and c-Myc were prominently induced. As a validation of this finding, T cell help was previously shown to induce expression of the proto-oncogene c-Myc (Calado et al., 2012; Dominguez-Sola et al., 2012). E2F is repressed by the Retinoblastoma (Rb) protein, and cyclin-dependent protein kinases (CDKs) de-repress E2F by phosphorylating Rb (Chellappan et al., 1991; Chen et al., 2009). Consistent with this, intracellular Rb phosphorylation was increased among selected GC B cells, corroborating the enhanced expression of E2F target genes in selected G1 DZ

cells. These findings prompted a re-evaluation of the cell cycle of selected GC B cells in greater detail. In particular, I sought to uncouple whether selected cells are able to divide a greater number of times only because they spend more time in the DZ, or whether selected cells might also undergo accelerated cell cycle rates during their prolonged residence time in the DZ.

Examining progression rates through the cell cycle has generally been accomplished by experimentally synchronizing cell populations in tissue culture with inhibitors of S phase or mitosis. Removal of the employed inhibitor allows the arrested cell population to be synchronously released into the same cell cycle phase. Following these cells over time, as they progress through the cell cycle, allows progression through distinct phases to be followed, measured and analyzed. However, no such exogenous agent can be applied to experimentally synchronize the cell cycle of GC B cells in vivo. Thus, examining the regulation of cell cycle dynamics during GC selection required the development of novel techniques.

To examine cell cycle dynamics in the GC, I utilized the sequential EdU/BrdU double-pulse technique to retrospectively “synchronize” GC B cells in a non-perturbing manner. To do so, the EdU/BrdU method was further combined with DNA content staining. Mice were intravenously injected first with EdU, then 1 hour later injected with BrdU, and then analyzed by DNA content at 0.5, 2.5, and

5 hours after the EdU/BrdU double-pulse. In this manner, cells in early, mid/late, or post-S phase periods of the cell cycle can be identified based on their incorporation patterns of EdU/BrdU and examined at time points thereafter for their rate of progression through S phase or completion of G2/M by DNA content. This new method of analyzing cell cycle dynamics in vivo, which should be generally applicable to a variety of physiological contexts, revealed that T cell help accelerates progression of selected GC B cells through both the S and G2/M phases of the cell cycle. Consistently, EdU labeling of anti-NP GCs in C57BL/6 revealed that affinity-enhancing mutations during the polyclonal immune response are associated with rapid progression through the S/G2/M phases.

4.3.1. Mechanism of S phase regulation during selection

Once a GC B cell has completed the G1/S transition, DNA replication occupies most of the time that it takes the cell to complete the cell cycle. Regulation of S phase duration is a well-known feature of embryonic development (Blumenthal et al., 1974; Collart et al., 2013; Hyrien et al., 1995; McKnight and Miller, 1977; Nordman and Orr-Weaver, 2012). This regulation is most dramatically seen during the midblastula transition (MBT), which marks the onset of zygotic transcription, morphogenesis, and embryonic cell movements. Coincident with these developmental changes, the cell cycle and DNA replication at the MBT are dramatically lengthened. Prior to the MBT, the rapid early cell cycles of the

embryo are fueled by maternally-derived gene products. As development proceeds beyond the MBT, DNA replication slows because replication initiation factors and CDK activity become limiting (Collart et al., 2013; Farrell et al., 2012). As a consequence, S phase in the later embryo involves activation of fewer origins that are fired asynchronously, whereas the earliest S phases are completed more rapidly due to their use of a larger number of origins that fire more synchronously. I therefore sought to determine whether T cell help might involve the use of a similar mechanism during GC B cell selection to accelerate S phase.

The dynamics of S phase initiation can be determined by sequencing the genomes of G1 and S phase cells (Koren et al., 2014; Koren et al., 2012). In this method, analyzing the relative copy number of sequences along chromosomes in S phase provides a view into the timing of replication of different genomic sites. Early sites of DNA replication, which are encompassed within or proximal to early-firing replication origins, will contain relatively higher copy number in a population of S phase cells than regions that are typically replicated later during S phase. However, these experiments revealed that selected GC B cells initiate S phase using the same locations and activation times of origins throughout the genome. Thus, although T cell help accelerates DNA replication, it does so without regulating the global replication timing program.

In tissue culture, DNA replication forks can be accelerated by coordinate activation of c-Myc, CDK activity and nucleotide metabolism (Anglana et al., 2003; Bester et al., 2011; Malinsky et al., 2001). Such regulation has not, however, been documented in a physiological context. Given the finding that T cell help mediates similar changes in selected GC B cells, I reasoned that similar changes to DNA replication fork speed might take place during the S phase of selected GC B cells. Therefore, single-molecule analyses of DNA replication were performed, which revealed that the speed of replication forks in GC B cells is increased during T cell-mediated selection.

The mechanism of T cell-mediated S phase regulation in the GC thus appears to differ fundamentally from developmental regulation of S phase. Whereas regulation of S phase length in the developing embryo appears to operate by passive dilution of limiting replication factors and activities (Collart et al., 2013), S phase regulation during GC selection is a consequence of directed signaling by T cells to selected GC B cells. The signals transduced by T cell help coordinately alter nucleotide metabolism, general cellular metabolism, and signaling pathways (c-Myc and CDK) that drive rapid entry into and progression through the cell cycle. Moreover, the rapid early S phases in development do not appear to involve faster replication forks, but rather involve synchronous use of a greater number of replication origins. In contrast, selected GC B cells accelerate their S phase by enhancing their rate of replication elongation while maintaining the

temporal order and number of replication initiation events throughout the genome. As the longest phase of the committed cell cycle, S phase thus provides a critical point of dynamic regulation during GC selection.

4.4. Model of affinity-based selection in the germinal center

Collectively, the results described in this thesis provide a coherent model of the dynamics of T cell-mediated selection in the GC. GC B cells capture and present antigen through their BCRs in an affinity-dependent manner, allowing higher affinity B cells to present a higher density of pMHCII and thus elicit T cell help of a proportionally greater magnitude (Gitlin et al., 2014; Shulman et al., 2014). T cells then transduce signals within selected GC B cells that direct their return to the DZ where they subsequently undergo preferential expansion by a twofold mechanism: (1) selected cells dwell for a prolonged period of time in the DZ and (2) undergo accelerated cell cycles therein. These two dynamic mechanisms thus work in concert, enabling high affinity B cells to selectively and rapidly expand within the GC population, thereby leading to affinity maturation of the antibody response.

Chapter 5:

Methods

5.1 Mice

C57BL/6, B6.SJL, Col1A1-tetO-H2B–mCherry and DsRed mice were purchased from Jackson Laboratories. Vav-tTA transgenic mice that had been backcrossed to C57/BL6 were obtained from S. W. Lowe and crossed to Col1A1-tetO-H2B–mCherry mice to produce tTA–H2B–mCh mice (Egli et al., 2007; Wiesner et al., 2005). B1-8^{hi}, DEC205$^{-/-}$, and PAGFP transgenic mice were described previously (Guo et al., 2000; Shih et al., 2002b; Victora et al., 2010). Fucci transgenic mice were obtained from T. Kurosaki and A. Miyawaki (Aiba et al., 2010; Sakaue-Sawano et al., 2008). All experiments were performed with authorization from the Institutional Review Board and the IACUC at The Rockefeller University.

5.2 B cell transfer and culture

Resting splenic B cells were purified by forcing mouse spleens through 40 μm mesh into complete RPMI media (Gibco) containing 6% serum. CD43 magnetic beads (MACS) were used to purify resting B cells from single cell suspensions,

according to manufacturer's protocols (Militenyi Biotec). All experiments involved adoptive transfers of 1.5-10 x10^6 B cells (≈(1.5-10) x 10^5 Igλ^+, NP-specific B cells) into recipient mice. To evaluate the tTA-H2B-mCh system during in vitro proliferation, resting B cells were purified from tTA-H2B-mCh mice and labeled at 37 °C in 5 μM CFSE. B cells were then stimulated in culture with lipopolysacchard and IL-4 for 72 hours, as described previously (Robbiani et al., 2008), in the presence of DOX (500 ng/ml).

5.3 Immunizations and treatments

C57BL/6 or B6.SJL mice (6-8 weeks of age) were primed by intraperitoneal immunization with 100 μl containing 50 μg of OVA (Grade V, Sigma) precipitated in alum at a 2:1 ratio. Two to six weeks later, mice received the indicated adoptive transfers followed by subcutaneous boosting with 25 μg of NP_{14}-OVA or NP_{16}-OVA (Biosearch Technologies) the following day. Draining lymph nodes were collected and processed for flow cytometry. To induce polyclonal GCs, C57BL/6 or tTA-H2B-mCh mice were immunized intraperitoneally with 50 μg of NP_{14}-OVA or NP_{16}-OVA in alum. To induce anti-gp120 GCs, tTA-H2B-mCh mice were immunized with 12.5 μg and 6.25 μg of HIV-1_{YU2} gp120 intraperitoneally and subcutaneously, respectively, in alum. αDEC-OVA and αDEC-CS fusion antibodies were produced by transient transfection in 293T cells, as described previously (Boscardin et al., 2006). 5 μg of fusion antibody in PBS was injected

subcutaneously at the indicated time points, except in Figures 2.1, 2.2, 2.6, 2.7, 2.10, 2.11, 2.12 where 10 μg of fusion antibody was used. Mice were administered DOX by intraperitoneal injection of 1.6 mg DOX (Sigma) in PBS and subcutaneous injection of 0.2 mg DOX in PBS. Maintenance on DOX was accomplished by adding DOX (2 mg/ml) and sucrose (10 mg/ml) to the drinking water for indicated time periods.

5.4 Cell cycle analysis

For cell cycle analysis in Figures 2.9, 3.4, 3.5, 3.6, 3.7, and 3.8, 1 mg EdU (Life Technologies) in PBS was injected intravenously followed 0.5 hours later by intravenous injection of 2 mg BrdU (Sigma-Aldrich) in PBS. Cells were then stained for flow cytometry and processed using an anti-BrdU-FITC kit (BD Biosciences) and Click-iT EdU-Pacific Blue kit (Life Technologies) according to manufacturers' instructions. DNA content was generally analyzed by staining cells with 7-AAD (BD Biosciences), or DAPI in other cases, to assess DNA content. In Figure 3.10, mice were treated with 1 mg EdU intravenously followed 0.5 hours later with 5 mg BrdU intraperitoneally. For DNA fiber analyses, mice were injected with 1.25 mg and 0.125 mg of IdU (Sigma-Aldrich) in PBS intraperitoneally and subcutaneously, respectively. Mice were then injected with 1 mg of thymidine (EMD Millipore) after 20 minutes immediately before processing lymph nodes for cell sorting.

5.5 Flow cytometry and cell sorting

Single cell suspensions from indicated tissues were processed in PBS that was maintained at 4°C and contained 2% serum and 1 mM EDTA. Samples were treated at 4°C for 10 minutes with 1 µg/ml of anti-CD16/32 (2.4G2, Bio-X-Cell) and then stained for 25-30 minutes at 4°C. Anti-B220, CD38, CD86, CD45.1, CD45.2 antibodies were from eBioscience. FAS, CXCR4, CD45.1, CD45.2, Igλ1-3, GL7, streptavidin-phycoerythrin and streptavidin-allophycocyanin were from BD Biosciences. Streptavidin-Alexa Fluor 488 was from Invitrogen. Antibody for intracellular staining of pRb-S807/811 was from Cell Signaling Technology (clone: D20B12). Cell fixation and permeabilization were performed using the Cytofix/Cytoperm kit (BD Biosciences). Samples were analyzed on a BD Fortessa. GC B cells were gated as live/single and $B220^+$ and either $CD38^-FAS^+$ or FAS^+GL7^+. DZ cells were gated as $CXCR4^{High}CD86^-$. CD45.1 and CD45.2 allotypic markers or DsRed were used to trace transferred B cell populations within recipient mice. B1-8^{hi} $DEC205^{+/+}$ B cells were identified as $CD45.1^+$, B1-8^{hi} $DEC205^{-/-}$ B cells were identified as $CD45.1^+CD45.2^+$, and B1-8^{hi} tTA-H2B-mCh B cells were identified as $CD45.2^+$. For RNA sequencing, cells were sorted directly into Trizol LS reagent (Invitrogen) maintained at 4°C using a FACS Aria II (Becton Dickinson). Prior to cell sorting in the experiment in Figure 3.10, GC B cells were enriched using anti-IgD-biotin (eBioscience) and both anti-biotin and CD43 magnetic beads (MACS).

5.6 Photoactivation

Intravital imaging and photoactivation were performed as described previously (Shulman et al., 2013; Victora et al., 2010). Anaesthesia was induced with 100 mg ketamine, 15 mg xylazine and 2.5 mg acepromazine per kg of body weight and maintained with 1.25% isoflurane in 100% oxygen. A double-edged razor blade was used to shave hind legs. Mice were restrained on a 37 °C stage warmer (BioTherm Micro S37; Biogenics) and an incision was made behind the knee to allow exposure of the popliteal lymph node. Once exposed, the lymph node was restrained with a metal strap and visualized with a microscope objective and a 40 °C objective heater. To visualize LZ-resident follicular dendritic cells, 1 μg of the fluorescent protein tdTomato conjugated to NP was injected into hind footpads one day prior to imaging, as described previously (Victora et al., 2010). To photoactivate DZ B cells in Figures 2.10, 2.11, and 2.12, B1-8^{hi} PAGFP^{+} GC B cells were photoactivated external to NP–tdTomato-labeled FDCs in the LZ by scanning with a femtosecond-pulsed multiphoton laser tuned to 820 nm wavelength and imaged at 940 nm wavelength, as previously described (Shulman et al., 2013; Victora et al., 2010). Cell motility was monitored immediately following photoactivation to ensure cell viability. Incisions were sutured and mice were allowed to recover for 6 hours before flow cytometry. To determine the precision of DZ photoactivation, lymph node cells were analyzed immediately after photoactivation by flow cytometry for surface phenotype.

Imaging experiments were performed with an Olympus BX61 upright microscope (Olympus ×25 1.05 NA Plan objective), fitted with a Coherent Chameleon Vision II laser (Rockefeller University Bio-Imaging Resource Center).

5.7 Gene expression analysis

Libraries were generated from purified RNA of sorted cells using the SMARTer Ultra Low Input RNA for Illumina Sequencing kit (Clontech Laboratories). High throughput sequencing was performed using a HiSeq 2500 (Illumina). RNA-seq reads were aligned with STAR version 2.3.0 allowing unique alignments and using Mouse Ensembl genes as reference. Differential expression was calculated using Cufflinks with default settings. Gene Set Enrichment Analyses were performed using GSEA v2.2.2.

5.8 Replication timing data

To generate replication timing profiles, single cell suspensions were stained for surface markers and fixed and permeabilized as described above. Samples were then incubated for 30 minutes in 100 μl of 20 μg/μl RNAse A (Life Technologies) at 37°C and then stained for DNA content with 7-AAD. B1-8^{hi} DEC205$^{+/+}$ GC B cells were sorted as B220^{+}CD38^{-} FAS^{+}CD45.1^{+}CD45.2^{-} and sorted based on either in G1 or S phase as determined by DNA content. Purified genomic DNA

from sorted cells was used to prepare libraries for sequencing on a HiSeq 2500 (Illumina). Sequence reads were aligned to the mouse reference genome, build mm9, using BWA mem with default settings. Replication timing was determined using normalized sequence tag density values for G1 and S for each 2 kb window of the genome. Only windows containing > 25% of tags expected by a uniform distribution throughout the genome were used. 2 kb window data were smoothed using the Matlab function Csaps with a parameter of 10^{-17}. Smoothed data for the two biological replicates of each condition were averaged, and both averaged and single-repeat data were Z-score normalized to a genome-wide mean of zero and standard deviation of 1. Smoothed data was compared to Mouse replication timing data from L1210 lymphoblast cells (Yaffe et al., 2010) were used to compare the smoothed data generated in this study by interpolating to the same data coordinates.

5.9 DNA Fiber analyses

DNA fibers analysis was performed on sorted GC B cells, as previously described (Jackson and Pombo, 1998). Sorted were re-suspended in PBS at $1x10^6$ cells/ml and 2 μl of cells were spotted onto a glass slide followed by 6 minutes of lysis in 10 μl spreading buffer (0.5% SDS in 200 mM TRIS-HCl (pH 7.4) and 50 mM EDTA). Slides were tilted at a 15° to extend DNA fibers. Slides were then air-dried and fixed in a 3:1 mixture of methanol and acetic acid for 2

minutes. 2.5 M HCl was then used to denature DNA for 25-30 minutes at room temperature. After washing in PBS, slides were blocked for 1 hour in PBS with 0.1% Triton X- 100 + 10% goat serum (MP Biomedicals 092939149). IdU-labeled tracks were detected using mouse anti-BrdU (Becton Dickinson 347580, 1:100) and Alexa Fluor 488-labelled goat anti-mouse IgG (InvitrogenA11029, 1:350) antibodies. DNA fibers were counterstained with anti-ssDNA (Millipore MAB3034, 1:600) and Alexa Fluor 647-labeled goat anti-mouse IgG2A (Invitrogen A21241, 1:350). Slides were mounted in Prolong Gold antifade reagent (Invitrogen) and replication tracks were imaged on a DeltaVision Elite system (Applied Precision) and measured using SoftWoRx software (Applied Precision).

5.10 V_H186.2 and J_H4 intron sequence analyses

Genomic DNA was extracted from GC B cells that were isolated as described in the indicated figures. PCR was performed using Phusion HF (New England Biolabs) from DNA corresponding to 1,000-5,000 cells. PCR amplification strategy for V_H186.2 analysis was performed as described previously (Dominguez-Sola et al., 2012; Victora et al., 2010). To amplify J_H4 intronic sequences, the following primers were used for 35 cycles with an annealing temperature of 57 °C and an extension time at 72 °C for 1 min: 5′-TCCTAGGAACCAACTTAAGAGT-3′ and 5′-TGGAGTTTTCTGAGCATTGCAG-3′. PCR products were gel-extracted and cloned into Zero Blunt TOPO vectors

(Invitrogen) as described previously. Antibody gene sequences were analyzed using the IMGT/V-QUEST system to identify W33L and K59R mutations. For mutational analysis of the J_H4 intron, high quality traces were analyzed using MacVector 12.7 for base-pair mismatches and deletions compared to the germline sequence. Both mismatches and deletions were counted as mutations. Mutation frequency was calculated by summing the total number of mutations from all clones analyzed in a given condition and dividing by the total number of base pairs analyzed in that group.

5.11 Statistical Analyses

Statistical significance was assessed with the tests indicated in the figures using Prism software v. 5.0 (Graphpad).

Chapter 6:

References

Aiba, Y., Kometani, K., Hamadate, M., Moriyama, S., Sakaue-Sawano, A., Tomura, M., Luche, H., Fehling, H.J., Casellas, R., Kanagawa, O.*, et al.* (2010). Preferential localization of IgG memory B cells adjacent to contracted germinal centers. Proceedings of the National Academy of Sciences of the United States of America *107*, 12192-12197.

Allen, C.D., Ansel, K.M., Low, C., Lesley, R., Tamamura, H., Fujii, N., and Cyster, J.G. (2004). Germinal center dark and light zone organization is mediated by CXCR4 and CXCR5. Nature immunology *5*, 943-952.

Allen, C.D., Okada, T., and Cyster, J.G. (2007a). Germinal-center organization and cellular dynamics. Immunity *27*, 190-202.

Allen, C.D., Okada, T., Tang, H.L., and Cyster, J.G. (2007b). Imaging of germinal center selection events during affinity maturation. Science *315*, 528-531.

Allen, D., Simon, T., Sablitzky, F., Rajewsky, K., and Cumano, A. (1988). Antibody engineering for the analysis of affinity maturation of an anti-hapten response. The EMBO journal *7*, 1995-2001.

Allen, R.C., Armitage, R.J., Conley, M.E., Rosenblatt, H., Jenkins, N.A., Copeland, N.G., Bedell, M.A., Edelhoff, S., Disteche, C.M., Simoneaux, D.K.*, et al.* (1993). CD40 ligand gene defects responsible for X-linked hyper-IgM syndrome. Science *259*, 990-993.

Amit, A.G., Mariuzza, R.A., Phillips, S.E., and Poljak, R.J. (1986). Three-dimensional structure of an antigen-antibody complex at 2.8 A resolution. Science *233*, 747-753.

Amzel, L.M., and Poljak, R.J. (1979). Three-dimensional structure of immunoglobulins. Annual review of biochemistry *48*, 961-997.

Anglana, M., Apiou, F., Bensimon, A., and Debatisse, M. (2003). Dynamics of DNA replication in mammalian somatic cells: nucleotide pool modulates origin choice and interorigin spacing. Cell *114*, 385-394.

Ansel, K.M., McHeyzer-Williams, L.J., Ngo, V.N., McHeyzer-Williams, M.G., and Cyster, J.G. (1999). In vivo-activated CD4 T cells upregulate CXC chemokine

receptor 5 and reprogram their response to lymphoid chemokines. The Journal of experimental medicine *190*, 1123-1134.

Bannard, O., Horton, R.M., Allen, C.D., An, J., Nagasawa, T., and Cyster, J.G. (2013). Germinal center centroblasts transition to a centrocyte phenotype according to a timed program and depend on the dark zone for effective selection. Immunity *39*, 912-924.

Batista, F.D., and Neuberger, M.S. (1998). Affinity dependence of the B cell response to antigen: a threshold, a ceiling, and the importance of off-rate. Immunity *8*, 751-759.

Batista, F.D., and Neuberger, M.S. (2000). B cells extract and present immobilized antigen: implications for affinity discrimination. The EMBO journal *19*, 513-520.

Berek, C., Berger, A., and Apel, M. (1991). Maturation of the immune response in germinal centers. Cell *67*, 1121-1129.

Berek, C., and Milstein, C. (1987). Mutation drift and repertoire shift in the maturation of the immune response. Immunological reviews *96*, 23-41.

Bester, A.C., Roniger, M., Oren, Y.S., Im, M.M., Sarni, D., Chaoat, M., Bensimon, A., Zamir, G., Shewach, D.S., and Kerem, B. (2011). Nucleotide deficiency promotes genomic instability in early stages of cancer development. Cell *145*, 435-446.

Blumenthal, A.B., Kriegstein, H.J., and Hogness, D.S. (1974). The units of DNA replication in Drosophila melanogaster chromosomes. Cold Spring Harbor symposia on quantitative biology *38*, 205-223.

Boes, M., Esau, C., Fischer, M.B., Schmidt, T., Carroll, M., and Chen, J. (1998). Enhanced B-1 cell development, but impaired IgG antibody responses in mice deficient in secreted IgM. J Immunol *160*, 4776-4787.

Boscardin, S.B., Hafalla, J.C., Masilamani, R.F., Kamphorst, A.O., Zebroski, H.A., Rai, U., Morrot, A., Zavala, F., Steinman, R.M., Nussenzweig, R.S.*, et al.* (2006). Antigen targeting to dendritic cells elicits long-lived T cell help for antibody responses. The Journal of experimental medicine *203*, 599-606.

Bransteitter, R., Pham, P., Scharff, M.D., and Goodman, M.F. (2003). Activation-induced cytidine deaminase deaminates deoxycytidine on single-stranded DNA but requires the action of RNase. Proceedings of the National Academy of Sciences of the United States of America *100*, 4102-4107.

Brown, M., Stenzel-Poore, M., Stevens, S., Kondoleon, S.K., Ng, J., Bachinger, H.P., and Rittenberg, M.B. (1992). Immunologic memory to phosphocholine keyhole limpet hemocyanin. Recurrent mutations in the lambda 1 light chain increase affinity for antigen. J Immunol *148*, 339-346.

Burnet, F.M. (1959). The clonal selection theory of acquired immunity (Nashville,: Vanderbilt University Press).

Calado, D.P., Sasaki, Y., Godinho, S.A., Pellerin, A., Kochert, K., Sleckman, B.P., de Alboran, I.M., Janz, M., Rodig, S., and Rajewsky, K. (2012). The cell-cycle regulator c-Myc is essential for the formation and maintenance of germinal centers. Nature immunology *13*, 1092-1100.

Carrasco, Y.R., and Batista, F.D. (2007). B cells acquire particulate antigen in a macrophage-rich area at the boundary between the follicle and the subcapsular sinus of the lymph node. Immunity *27*, 160-171.

Casellas, R., Shih, T.A., Kleinewietfeld, M., Rakonjac, J., Nemazee, D., Rajewsky, K., and Nussenzweig, M.C. (2001). Contribution of receptor editing to the antibody repertoire. Science *291*, 1541-1544.

Chaudhuri, J., Tian, M., Khuong, C., Chua, K., Pinaud, E., and Alt, F.W. (2003). Transcription-targeted DNA deamination by the AID antibody diversification enzyme. Nature *422*, 726-730.

Chellappan, S.P., Hiebert, S., Mudryj, M., Horowitz, J.M., and Nevins, J.R. (1991). The E2F transcription factor is a cellular target for the RB protein. Cell *65*, 1053-1061.

Chen, H.Z., Tsai, S.Y., and Leone, G. (2009). Emerging roles of E2Fs in cancer: an exit from cell cycle control. Nature reviews Cancer *9*, 785-797.

Chen, Z., Koralov, S.B., Gendelman, M., Carroll, M.C., and Kelsoe, G. (2000). Humoral immune responses in Cr2-/- mice: enhanced affinity maturation but impaired antibody persistence. J Immunol *164*, 4522-4532.

Collart, C., Allen, G.E., Bradshaw, C.R., Smith, J.C., and Zegerman, P. (2013). Titration of four replication factors is essential for the Xenopus laevis midblastula transition. Science *341*, 893-896.

Craxton, A., Otipoby, K.L., Jiang, A., and Clark, E.A. (1999). Signal transduction pathways that regulate the fate of B lymphocytes. Advances in immunology *73*, 79-152.

Dal Porto, J.M., Haberman, A.M., Kelsoe, G., and Shlomchik, M.J. (2002). Very low affinity B cells form germinal centers, become memory B cells, and participate in secondary immune responses when higher affinity competition is reduced. The Journal of experimental medicine *195*, 1215-1221.

Dang, C.V. (2012). MYC on the path to cancer. Cell *149*, 22-35.

de Vinuesa, C.G., Cook, M.C., Ball, J., Drew, M., Sunners, Y., Cascalho, M., Wabl, M., Klaus, G.G., and MacLennan, I.C. (2000). Germinal centers without T cells. The Journal of experimental medicine *191*, 485-494.

Deenick, E.K., Hasbold, J., and Hodgkin, P.D. (1999). Switching to IgG3, IgG2b, and IgA is division linked and independent, revealing a stochastic framework for describing differentiation. J Immunol *163*, 4707-4714.

Depoil, D., Zaru, R., Guiraud, M., Chauveau, A., Harriague, J., Bismuth, G., Utzny, C., Muller, S., and Valitutti, S. (2005). Immunological synapses are versatile structures enabling selective T cell polarization. Immunity *22*, 185-194.

Di Noia, J.M., and Neuberger, M.S. (2007). Molecular mechanisms of antibody somatic hypermutation. Annual review of biochemistry *76*, 1-22.

Dickerson, S.K., Market, E., Besmer, E., and Papavasiliou, F.N. (2003). AID mediates hypermutation by deaminating single stranded DNA. The Journal of experimental medicine *197*, 1291-1296.

Dominguez-Sola, D., and Gautier, J. (2014). MYC and the control of DNA replication. Cold Spring Harbor perspectives in medicine *4*.

Dominguez-Sola, D., Victora, G.D., Ying, C.Y., Phan, R.T., Saito, M., Nussenzweig, M.C., and Dalla-Favera, R. (2012). The proto-oncogene MYC is required for selection in the germinal center and cyclic reentry. Nature immunology *13*, 1083-1091.

Egli, D., Rosains, J., Birkhoff, G., and Eggan, K. (2007). Developmental reprogramming after chromosome transfer into mitotic mouse zygotes. Nature *447*, 679-685.

Eisen, H.N., and Siskind, G.W. (1964). Variations in Affinities of Antibodies during the Immune Response. Biochemistry *3*, 996-1008.

Farrell, J.A., Shermoen, A.W., Yuan, K., and O'Farrell, P.H. (2012). Embryonic onset of late replication requires Cdc25 down-regulation. Genes & development *26*, 714-725.

Ferrari, S., Giliani, S., Insalaco, A., Al-Ghonaium, A., Soresina, A.R., Loubser, M., Avanzini, M.A., Marconi, M., Badolato, R., Ugazio, A.G.*, et al.* (2001). Mutations of CD40 gene cause an autosomal recessive form of immunodeficiency with hyper IgM. Proceedings of the National Academy of Sciences of the United States of America *98*, 12614-12619.

Foudi, A., Hochedlinger, K., Van Buren, D., Schindler, J.W., Jaenisch, R., Carey, V., and Hock, H. (2009). Analysis of histone 2B-GFP retention reveals slowly cycling hematopoietic stem cells. Nature biotechnology *27*, 84-90.

Furukawa, K., Akasako-Furukawa, A., Shirai, H., Nakamura, H., and Azuma, T. (1999). Junctional amino acids determine the maturation pathway of an antibody. Immunity *11*, 329-338.

Garside, P., Ingulli, E., Merica, R.R., Johnson, J.G., Noelle, R.J., and Jenkins, M.K. (1998). Visualization of specific B and T lymphocyte interactions in the lymph node. Science *281*, 96-99.

Gauld, S.B., Dal Porto, J.M., and Cambier, J.C. (2002). B cell antigen receptor signaling: roles in cell development and disease. Science *296*, 1641-1642.

Gay, D., Saunders, T., Camper, S., and Weigert, M. (1993). Receptor editing: an approach by autoreactive B cells to escape tolerance. The Journal of experimental medicine *177*, 999-1008.

Gitlin, A.D., and Nussenzweig, M.C. (2015). Immunology: Fifty years of B lymphocytes. Nature *517*, 139-141.

Gitlin, A.D., Shulman, Z., and Nussenzweig, M.C. (2014). Clonal selection in the germinal centre by regulated proliferation and hypermutation. Nature *509*, 637-640.

Goidl, E.A., Paul, W.E., Siskind, G.W., and Benacerraf, B. (1968). The effect of antigen dose and time after immunization on the amount and affinity of anti-hapten antibody. J Immunol *100*, 371-375.

Gong, S., and Nussenzweig, M.C. (1996). Regulation of an early developmental checkpoint in the B cell pathway by Ig beta. Science *272*, 411-414.

Goodnow, C.C., Crosbie, J., Adelstein, S., Lavoie, T.B., Smith-Gill, S.J., Brink, R.A., Pritchard-Briscoe, H., Wotherspoon, J.S., Loblay, R.H., Raphael, K.*, et al.* (1988). Altered immunoglobulin expression and functional silencing of self-reactive B lymphocytes in transgenic mice. Nature *334*, 676-682.

Goodnow, C.C., Crosbie, J., Jorgensen, H., Brink, R.A., and Basten, A. (1989). Induction of self-tolerance in mature peripheral B lymphocytes. Nature *342*, 385-391.

Gu, H., Zou, Y.R., and Rajewsky, K. (1993). Independent control of immunoglobulin switch recombination at individual switch regions evidenced through Cre-loxP-mediated gene targeting. Cell *73*, 1155-1164.

Guo, M., Gong, S., Maric, S., Misulovin, Z., Pack, M., Mahnke, K., Nussenzweig, M.C., and Steinman, R.M. (2000). A monoclonal antibody to the DEC-205 endocytosis receptor on human dendritic cells. Human immunology *61*, 729-738.

Han, S., Hathcock, K., Zheng, B., Kepler, T.B., Hodes, R., and Kelsoe, G. (1995a). Cellular interaction in germinal centers. Roles of CD40 ligand and B7-2 in established germinal centers. J Immunol *155*, 556-567.

Han, S., Zheng, B., Dal Porto, J., and Kelsoe, G. (1995b). In situ studies of the primary immune response to (4-hydroxy-3-nitrophenyl)acetyl. IV. Affinity-dependent, antigen-driven B cell apoptosis in germinal centers as a mechanism for maintaining self-tolerance. The Journal of experimental medicine *182*, 1635-1644.

Hanna, M.G., Jr. (1964). An Autoradiographic Study of the Germinal Center in Spleen White Pulp during Early Intervals of the Immune Response. Laboratory investigation; a journal of technical methods and pathology *13*, 95-104.

Hannum, L.G., Haberman, A.M., Anderson, S.M., and Shlomchik, M.J. (2000). Germinal center initiation, variable gene region hypermutation, and mutant B cell selection without detectable immune complexes on follicular dendritic cells. The Journal of experimental medicine *192*, 931-942.

Hartley, S.B., Crosbie, J., Brink, R., Kantor, A.B., Basten, A., and Goodnow, C.C. (1991). Elimination from peripheral lymphoid tissues of self-reactive B lymphocytes recognizing membrane-bound antigens. Nature *353*, 765-769.

Harwood, N.E., and Batista, F.D. (2010). Early events in B cell activation. Annual review of immunology *28*, 185-210.

Hasbold, J., Lyons, A.B., Kehry, M.R., and Hodgkin, P.D. (1998). Cell division number regulates IgG1 and IgE switching of B cells following stimulation by CD40 ligand and IL-4. European journal of immunology *28*, 1040-1051.

Hauser, A.E., Junt, T., Mempel, T.R., Sneddon, M.W., Kleinstein, S.H., Henrickson, S.E., von Andrian, U.H., Shlomchik, M.J., and Haberman, A.M.

(2007). Definition of germinal-center B cell migration in vivo reveals predominant intrazonal circulation patterns. Immunity *26*, 655-667.

Haynes, N.M., Allen, C.D., Lesley, R., Ansel, K.M., Killeen, N., and Cyster, J.G. (2007). Role of CXCR5 and CCR7 in follicular Th cell positioning and appearance of a programmed cell death gene-1high germinal center-associated subpopulation. J Immunol *179*, 5099-5108.

Hermanson, G.G., Eisenberg, D., Kincade, P.W., and Wall, R. (1988). B29: a member of the immunoglobulin gene superfamily exclusively expressed on beta-lineage cells. Proceedings of the National Academy of Sciences of the United States of America *85*, 6890-6894.

Hodgkin, P.D., Lee, J.H., and Lyons, A.B. (1996). B cell differentiation and isotype switching is related to division cycle number. The Journal of experimental medicine *184*, 277-281.

Hombach, J., Tsubata, T., Leclercq, L., Stappert, H., and Reth, M. (1990). Molecular components of the B-cell antigen receptor complex of the IgM class. Nature *343*, 760-762.

Hozumi, N., and Tonegawa, S. (1976). Evidence for somatic rearrangement of immunoglobulin genes coding for variable and constant regions. Proceedings of the National Academy of Sciences of the United States of America *73*, 3628-3632.

Hyrien, O., Maric, C., and Mechali, M. (1995). Transition in specification of embryonic metazoan DNA replication origins. Science *270*, 994-997.

Jackson, D.A., and Pombo, A. (1998). Replicon clusters are stable units of chromosome structure: evidence that nuclear organization contributes to the efficient activation and propagation of S phase in human cells. The Journal of cell biology *140*, 1285-1295.

Jacob, J., Kassir, R., and Kelsoe, G. (1991a). In situ studies of the primary immune response to (4-hydroxy-3-nitrophenyl)acetyl. I. The architecture and dynamics of responding cell populations. The Journal of experimental medicine *173*, 1165-1175.

Jacob, J., Kelsoe, G., Rajewsky, K., and Weiss, U. (1991b). Intraclonal generation of antibody mutants in germinal centres. Nature *354*, 389-392.

Jacobson, E.B., Caporale, L.H., and Thorbecke, G.J. (1974). Effect of thymus cell injections on germinal center formation in lymphoid tissues of nude (thymusless) mice. Cellular immunology *13*, 416-430.

Jiang, W., Swiggard, W.J., Heufler, C., Peng, M., Mirza, A., Steinman, R.M., and Nussenzweig, M.C. (1995). The receptor DEC-205 expressed by dendritic cells and thymic epithelial cells is involved in antigen processing. Nature *375*, 151-155.

Jolly, C.J., Klix, N., and Neuberger, M.S. (1997). Rapid methods for the analysis of immunoglobulin gene hypermutation: application to transgenic and gene targeted mice. Nucleic acids research *25*, 1913-1919.

Jones, P.T., Dear, P.H., Foote, J., Neuberger, M.S., and Winter, G. (1986). Replacing the complementarity-determining regions in a human antibody with those from a mouse. Nature *321*, 522-525.

Junt, T., Moseman, E.A., Iannacone, M., Massberg, S., Lang, P.A., Boes, M., Fink, K., Henrickson, S.E., Shayakhmetov, D.M., Di Paolo, N.C*., et al.* (2007). Subcapsular sinus macrophages in lymph nodes clear lymph-borne viruses and present them to antiviral B cells. Nature *450*, 110-114.

Kamphorst, A.O., Guermonprez, P., Dudziak, D., and Nussenzweig, M.C. (2010). Route of antigen uptake differentially impacts presentation by dendritic cells and activated monocytes. J Immunol *185*, 3426-3435.

Kepler, T.B., and Perelson, A.S. (1993). Cyclic re-entry of germinal center B cells and the efficiency of affinity maturation. Immunology today *14*, 412-415.

Khalil, A.M., Cambier, J.C., and Shlomchik, M.J. (2012). B cell receptor signal transduction in the GC is short-circuited by high phosphatase activity. Science *336*, 1178-1181.

Kitamura, D., Kudo, A., Schaal, S., Muller, W., Melchers, F., and Rajewsky, K. (1992). A critical role of lambda 5 protein in B cell development. Cell *69*, 823-831.

Kitamura, D., and Rajewsky, K. (1992). Targeted disruption of mu chain membrane exon causes loss of heavy-chain allelic exclusion. Nature *356*, 154-156.

Kitamura, D., Roes, J., Kuhn, R., and Rajewsky, K. (1991). A B cell-deficient mouse by targeted disruption of the membrane exon of the immunoglobulin mu chain gene. Nature *350*, 423-426.

Klein, F., Diskin, R., Scheid, J.F., Gaebler, C., Mouquet, H., Georgiev, I.S., Pancera, M., Zhou, T., Incesu, R.B., Fu, B.Z., *et al.* (2013). Somatic mutations of the immunoglobulin framework are generally required for broad and potent HIV-1 neutralization. Cell *153*, 126-138.

Kocks, C., and Rajewsky, K. (1988). Stepwise intraclonal maturation of antibody affinity through somatic hypermutation. Proceedings of the National Academy of Sciences of the United States of America *85*, 8206-8210.

Koren, A., Handsaker, R.E., Kamitaki, N., Karlic, R., Ghosh, S., Polak, P., Eggan, K., and McCarroll, S.A. (2014). Genetic variation in human DNA replication timing. Cell *159*, 1015-1026.

Koren, A., Polak, P., Nemesh, J., Michaelson, J.J., Sebat, J., Sunyaev, S.R., and McCarroll, S.A. (2012). Differential relationship of DNA replication timing to different forms of human mutation and variation. American journal of human genetics *91*, 1033-1040.

Kraal, G., Breel, M., Janse, M., and Bruin, G. (1986). Langerhans' cells, veiled cells, and interdigitating cells in the mouse recognized by a monoclonal antibody. The Journal of experimental medicine *163*, 981-997.

Kraus, M., Alimzhanov, M.B., Rajewsky, N., and Rajewsky, K. (2004). Survival of resting mature B lymphocytes depends on BCR signaling via the Igalpha/beta heterodimer. Cell *117*, 787-800.

Kurosaki, T. (1999). Genetic analysis of B cell antigen receptor signaling. Annual review of immunology *17*, 555-592.

Kurosaki, T., Shinohara, H., and Baba, Y. (2010). B cell signaling and fate decision. Annual review of immunology *28*, 21-55.

Lam, K.P., Kuhn, R., and Rajewsky, K. (1997). In vivo ablation of surface immunoglobulin on mature B cells by inducible gene targeting results in rapid cell death. Cell *90*, 1073-1083.

Liu, Y.J., Joshua, D.E., Williams, G.T., Smith, C.A., Gordon, J., and MacLennan, I.C. (1989). Mechanism of antigen-driven selection in germinal centres. Nature *342*, 929-931.

Liu, Y.J., Zhang, J., Lane, P.J., Chan, E.Y., and MacLennan, I.C. (1991). Sites of specific B cell activation in primary and secondary responses to T cell-dependent and T cell-independent antigens. European journal of immunology *21*, 2951-2962.

MacLennan, I.C. (1994). Germinal centers. Annual review of immunology *12*, 117-139.

Malinsky, J., Koberna, K., Stanek, D., Masata, M., Votruba, I., and Raska, I. (2001). The supply of exogenous deoxyribonucleotides accelerates the speed of the replication fork in early S-phase. Journal of cell science *114*, 747-750.

Mandel, T.E., Phipps, R.P., Abbot, A., and Tew, J.G. (1980). The follicular dendritic cell: long term antigen retention during immunity. Immunological reviews *53*, 29-59.

Mandel, T.E., Phipps, R.P., Abbot, A.P., and Tew, J.G. (1981). Long-term antigen retention by dendritic cells in the popliteal lymph node of immunized mice. Immunology *43*, 353-362.

Matsumoto, M., Lo, S.F., Carruthers, C.J., Min, J., Mariathasan, S., Huang, G., Plas, D.R., Martin, S.M., Geha, R.S., Nahm, M.H.*, et al.* (1996). Affinity maturation without germinal centres in lymphotoxin-alpha-deficient mice. Nature *382*, 462-466.

McCall, M.N., and Hodgkin, P.D. (1999). Switch recombination and germ-line transcription are division-regulated events in B lymphocytes. Biochimica et biophysica acta *1447*, 43-50.

McKean, D., Huppi, K., Bell, M., Staudt, L., Gerhard, W., and Weigert, M. (1984). Generation of antibody diversity in the immune response of BALB/c mice to influenza virus hemagglutinin. Proceedings of the National Academy of Sciences of the United States of America *81*, 3180-3184.

McKnight, S.L., and Miller, O.L., Jr. (1977). Electron microscopic analysis of chromatin replication in the cellular blastoderm Drosophila melanogaster embryo. Cell *12*, 795-804.

Meffre, E., Casellas, R., and Nussenzweig, M.C. (2000). Antibody regulation of B cell development. Nature immunology *1*, 379-385.

Moriyama, S., Takahashi, N., Green, J.A., Hori, S., Kubo, M., Cyster, J.G., and Okada, T. (2014). Sphingosine-1-phosphate receptor 2 is critical for follicular helper T cell retention in germinal centers. The Journal of experimental medicine *211*, 1297-1305.

Muramatsu, M., Kinoshita, K., Fagarasan, S., Yamada, S., Shinkai, Y., and Honjo, T. (2000). Class switch recombination and hypermutation require

activation-induced cytidine deaminase (AID), a potential RNA editing enzyme. Cell *102*, 553-563.

Muramatsu, M., Sankaranand, V.S., Anant, S., Sugai, M., Kinoshita, K., Davidson, N.O., and Honjo, T. (1999). Specific expression of activation-induced cytidine deaminase (AID), a novel member of the RNA-editing deaminase family in germinal center B cells. The Journal of biological chemistry *274*, 18470-18476.

Nemazee, D.A., and Burki, K. (1989). Clonal deletion of B lymphocytes in a transgenic mouse bearing anti-MHC class I antibody genes. Nature *337*, 562-566.

Nieuwenhuis, P., and Opstelten, D. (1984). Functional anatomy of germinal centers. The American journal of anatomy *170*, 421-435.

Nordman, J., and Orr-Weaver, T.L. (2012). Regulation of DNA replication during development. Development *139*, 455-464.

Nussenzweig, V., and Benacerraf, B. (1967). Antihapten antibody specificity and L chain type. The Journal of experimental medicine *126*, 727-743.

Okada, T., Miller, M.J., Parker, I., Krummel, M.F., Neighbors, M., Hartley, S.B., O'Garra, A., Cahalan, M.D., and Cyster, J.G. (2005). Antigen-engaged B cells undergo chemotaxis toward the T zone and form motile conjugates with helper T cells. PLoS biology *3*, e150.

Oprea, M., and Perelson, A.S. (1997). Somatic mutation leads to efficient affinity maturation when centrocytes recycle back to centroblasts. J Immunol *158*, 5155-5162.

Pape, K.A., Catron, D.M., Itano, A.A., and Jenkins, M.K. (2007). The humoral immune response is initiated in lymph nodes by B cells that acquire soluble antigen directly in the follicles. Immunity *26*, 491-502.

Patterson, G.H., and Lippincott-Schwartz, J. (2002). A photoactivatable GFP for selective photolabeling of proteins and cells. Science *297*, 1873-1877.

Paus, D., Phan, T.G., Chan, T.D., Gardam, S., Basten, A., and Brink, R. (2006). Antigen recognition strength regulates the choice between extrafollicular plasma cell and germinal center B cell differentiation. The Journal of experimental medicine *203*, 1081-1091.

Peled, J.U., Kuang, F.L., Iglesias-Ussel, M.D., Roa, S., Kalis, S.L., Goodman, M.F., and Scharff, M.D. (2008). The biochemistry of somatic hypermutation. Annual review of immunology *26*, 481-511.

Pham, P., Bransteitter, R., Petruska, J., and Goodman, M.F. (2003). Processive AID-catalysed cytosine deamination on single-stranded DNA simulates somatic hypermutation. Nature *424*, 103-107.

Phan, T.G., Grigorova, I., Okada, T., and Cyster, J.G. (2007). Subcapsular encounter and complement-dependent transport of immune complexes by lymph node B cells. Nature immunology *8*, 992-1000.

Pincetic, A., Bournazos, S., DiLillo, D.J., Maamary, J., Wang, T.T., Dahan, R., Fiebiger, B.M., and Ravetch, J.V. (2014). Type I and type II Fc receptors regulate innate and adaptive immunity. Nature immunology *15*, 707-716.

Pulendran, B., Kannourakis, G., Nouri, S., Smith, K.G., and Nossal, G.J. (1995). Soluble antigen can cause enhanced apoptosis of germinal-centre B cells. Nature *375*, 331-334.

Rajewsky, K. (1996). Clonal selection and learning in the antibody system. Nature *381*, 751-758.

Ramiro, A.R., Stavropoulos, P., Jankovic, M., and Nussenzweig, M.C. (2003). Transcription enhances AID-mediated cytidine deamination by exposing single-stranded DNA on the nontemplate strand. Nature immunology *4*, 452-456.

Reif, K., Ekland, E.H., Ohl, L., Nakano, H., Lipp, M., Forster, R., and Cyster, J.G. (2002). Balanced responsiveness to chemoattractants from adjacent zones determines B-cell position. Nature *416*, 94-99.

Reina-San-Martin, B., Difilippantonio, S., Hanitsch, L., Masilamani, R.F., Nussenzweig, A., and Nussenzweig, M.C. (2003). H2AX is required for recombination between immunoglobulin switch regions but not for intra-switch region recombination or somatic hypermutation. The Journal of experimental medicine *197*, 1767-1778.

Reth, M. (1989). Antigen receptor tail clue. Nature *338*, 383-384.

Reth, M., and Wienands, J. (1997). Initiation and processing of signals from the B cell antigen receptor. Annual review of immunology *15*, 453-479.

Revy, P., Muto, T., Levy, Y., Geissmann, F., Plebani, A., Sanal, O., Catalan, N., Forveille, M., Dufourcq-Labelouse, R., Gennery, A.*, et al.* (2000). Activation-

induced cytidine deaminase (AID) deficiency causes the autosomal recessive form of the Hyper-IgM syndrome (HIGM2). Cell *102*, 565-575.

Robbiani, D.F., Bothmer, A., Callen, E., Reina-San-Martin, B., Dorsett, Y., Difilippantonio, S., Bolland, D.J., Chen, H.T., Corcoran, A.E., Nussenzweig, A.*, et al.* (2008). AID is required for the chromosomal breaks in c-myc that lead to c-myc/IgH translocations. Cell *135*, 1028-1038.

Roozendaal, R., Mempel, T.R., Pitcher, L.A., Gonzalez, S.F., Verschoor, A., Mebius, R.E., von Andrian, U.H., and Carroll, M.C. (2009). Conduits mediate transport of low-molecular-weight antigen to lymph node follicles. Immunity *30*, 264-276.

Russell, D.M., Dembic, Z., Morahan, G., Miller, J.F., Burki, K., and Nemazee, D. (1991). Peripheral deletion of self-reactive B cells. Nature *354*, 308-311.

Sakaguchi, N., Kashiwamura, S., Kimoto, M., Thalmann, P., and Melchers, F. (1988). B lymphocyte lineage-restricted expression of mb-1, a gene with CD3-like structural properties. The EMBO journal *7*, 3457-3464.

Sakaue-Sawano, A., Kurokawa, H., Morimura, T., Hanyu, A., Hama, H., Osawa, H., Kashiwagi, S., Fukami, K., Miyata, T., Miyoshi, H.*, et al.* (2008). Visualizing spatiotemporal dynamics of multicellular cell-cycle progression. Cell *132*, 487-498.

Sanchez, M., Misulovin, Z., Burkhardt, A.L., Mahajan, S., Costa, T., Franke, R., Bolen, J.B., and Nussenzweig, M. (1993). Signal transduction by immunoglobulin is mediated through Ig alpha and Ig beta. The Journal of experimental medicine *178*, 1049-1055.

Scheid, J.F., Mouquet, H., Feldhahn, N., Seaman, M.S., Velinzon, K., Pietzsch, J., Ott, R.G., Anthony, R.M., Zebroski, H., Hurley, A.*, et al.* (2009). Broad diversity of neutralizing antibodies isolated from memory B cells in HIV-infected individuals. Nature *458*, 636-640.

Scheid, J.F., Mouquet, H., Ueberheide, B., Diskin, R., Klein, F., Oliveira, T.Y., Pietzsch, J., Fenyo, D., Abadir, A., Velinzon, K.*, et al.* (2011). Sequence and structural convergence of broad and potent HIV antibodies that mimic CD4 binding. Science *333*, 1633-1637.

Schwickert, T.A., Lindquist, R.L., Shakhar, G., Livshits, G., Skokos, D., Kosco-Vilbois, M.H., Dustin, M.L., and Nussenzweig, M.C. (2007). In vivo imaging of germinal centres reveals a dynamic open structure. Nature *446*, 83-87.

Schwickert, T.A., Victora, G.D., Fooksman, D.R., Kamphorst, A.O., Mugnier, M.R., Gitlin, A.D., Dustin, M.L., and Nussenzweig, M.C. (2011). A dynamic T cell-limited checkpoint regulates affinity-dependent B cell entry into the germinal center. The Journal of experimental medicine *208*, 1243-1252.

Shaw, A.C., Mitchell, R.N., Weaver, Y.K., Campos-Torres, J., Abbas, A.K., and Leder, P. (1990). Mutations of immunoglobulin transmembrane and cytoplasmic domains: effects on intracellular signaling and antigen presentation. Cell *63*, 381-392.

Shih, T.A., Meffre, E., Roederer, M., and Nussenzweig, M.C. (2002a). Role of BCR affinity in T cell dependent antibody responses in vivo. Nature immunology *3*, 570-575.

Shih, T.A., Roederer, M., and Nussenzweig, M.C. (2002b). Role of antigen receptor affinity in T cell-independent antibody responses in vivo. Nature immunology *3*, 399-406.

Shokat, K.M., and Goodnow, C.C. (1995). Antigen-induced B-cell death and elimination during germinal-centre immune responses. Nature *375*, 334-338.

Shulman, Z., Gitlin, A.D., Targ, S., Jankovic, M., Pasqual, G., Nussenzweig, M.C., and Victora, G.D. (2013). T follicular helper cell dynamics in germinal centers. Science *341*, 673-677.

Shulman, Z., Gitlin, A.D., Weinstein, J.S., Lainez, B., Esplugues, E., Flavell, R.A., Craft, J.E., and Nussenzweig, M.C. (2014). Dynamic signaling by T follicular helper cells during germinal center B cell selection. Science *345*, 1058-1062.

Smith, K.G., Light, A., Nossal, G.J., and Tarlinton, D.M. (1997). The extent of affinity maturation differs between the memory and antibody-forming cell compartments in the primary immune response. The EMBO journal *16*, 2996-3006.

Sohail, A., Klapacz, J., Samaranayake, M., Ullah, A., and Bhagwat, A.S. (2003). Human activation-induced cytidine deaminase causes transcription-dependent, strand-biased C to U deaminations. Nucleic acids research *31*, 2990-2994.

Srinivasan, L., Sasaki, Y., Calado, D.P., Zhang, B., Paik, J.H., DePinho, R.A., Kutok, J.L., Kearney, J.F., Otipoby, K.L., and Rajewsky, K. (2009). PI3 kinase signals BCR-dependent mature B cell survival. Cell *139*, 573-586.

Stavnezer, J., Guikema, J.E., and Schrader, C.E. (2008). Mechanism and regulation of class switch recombination. Annual review of immunology *26*, 261-292.

Talmage, D.W. (1959). Immunological specificity, unique combinations of selected natural globulins provide an alternative to the classical concept. Science *129*, 1643-1648.

Tarlinton, D., and Good-Jacobson, K. (2013). Diversity among memory B cells: origin, consequences, and utility. Science *341*, 1205-1211.

Tiegs, S.L., Russell, D.M., and Nemazee, D. (1993). Receptor editing in self-reactive bone marrow B cells. The Journal of experimental medicine *177*, 1009-1020.

Tiller, T., Tsuiji, M., Yurasov, S., Velinzon, K., Nussenzweig, M.C., and Wardemann, H. (2007). Autoreactivity in human IgG+ memory B cells. Immunity *26*, 205-213.

Tonegawa, S. (1983). Somatic generation of antibody diversity. Nature *302*, 575-581.

Torres, R.M., Flaswinkel, H., Reth, M., and Rajewsky, K. (1996). Aberrant B cell development and immune response in mice with a compromised BCR complex. Science *272*, 1804-1808.

Tumbar, T., Guasch, G., Greco, V., Blanpain, C., Lowry, W.E., Rendl, M., and Fuchs, E. (2004). Defining the epithelial stem cell niche in skin. Science *303*, 359-363.

Victora, G.D., and Nussenzweig, M.C. (2012). Germinal centers. Annual review of immunology *30*, 429-457.

Victora, G.D., Schwickert, T.A., Fooksman, D.R., Kamphorst, A.O., Meyer-Hermann, M., Dustin, M.L., and Nussenzweig, M.C. (2010). Germinal center dynamics revealed by multiphoton microscopy with a photoactivatable fluorescent reporter. Cell *143*, 592-605.

Wagner, S.D., Milstein, C., and Neuberger, M.S. (1995). Codon bias targets mutation. Nature *376*, 732.

Walker, L.M., Phogat, S.K., Chan-Hui, P.Y., Wagner, D., Phung, P., Goss, J.L., Wrin, T., Simek, M.D., Fling, S., Mitcham, J.L.*, et al.* (2009). Broad and potent

neutralizing antibodies from an African donor reveal a new HIV-1 vaccine target. Science *326*, 285-289.

Wardemann, H., Yurasov, S., Schaefer, A., Young, J.W., Meffre, E., and Nussenzweig, M.C. (2003). Predominant autoantibody production by early human B cell precursors. Science *301*, 1374-1377.

Weigert, M.G., Cesari, I.M., Yonkovich, S.J., and Cohn, M. (1970). Variability in the lambda light chain sequences of mouse antibody. Nature *228*, 1045-1047.

West, A.P., Jr., Scharf, L., Scheid, J.F., Klein, F., Bjorkman, P.J., and Nussenzweig, M.C. (2014a). Structural Insights on the Role of Antibodies in HIV-1 Vaccine and Therapy. Cell *156*, 633-648.

West, A.P., Jr., Scharf, L., Scheid, J.F., Klein, F., Bjorkman, P.J., and Nussenzweig, M.C. (2014b). Structural insights on the role of antibodies in HIV-1 vaccine and therapy. Cell *156*, 633-648.

Wiesner, S.M., Jones, J.M., Hasz, D.E., and Largaespada, D.A. (2005). Repressible transgenic model of NRAS oncogene-driven mast cell disease in the mouse. Blood *106*, 1054-1062.

Williams, G.T., Peaker, C.J., Patel, K.J., and Neuberger, M.S. (1994). The alpha/beta sheath and its cytoplasmic tyrosines are required for signaling by the B-cell antigen receptor but not for capping or for serine/threonine-kinase recruitment. Proceedings of the National Academy of Sciences of the United States of America *91*, 474-478.

Wu, X., Jiang, N., Fang, Y.F., Xu, C., Mao, D., Singh, J., Fu, Y.X., and Molina, H. (2000). Impaired affinity maturation in Cr2-/- mice is rescued by adjuvants without improvement in germinal center development. J Immunol *165*, 3119-3127.

Wu, X., Yang, Z.Y., Li, Y., Hogerkorp, C.M., Schief, W.R., Seaman, M.S., Zhou, T., Schmidt, S.D., Wu, L., Xu, L.*, et al.* (2010). Rational design of envelope identifies broadly neutralizing human monoclonal antibodies to HIV-1. Science *329*, 856-861.

Xiao, X., Chen, W., Feng, Y., Zhu, Z., Prabakaran, P., Wang, Y., Zhang, M.Y., Longo, N.S., and Dimitrov, D.S. (2009). Germline-like predecessors of broadly neutralizing antibodies lack measurable binding to HIV-1 envelope glycoproteins: implications for evasion of immune responses and design of vaccine immunogens. Biochemical and biophysical research communications *390*, 404-409.

Yaffe, E., Farkash-Amar, S., Polten, A., Yakhini, Z., Tanay, A., and Simon, I. (2010). Comparative analysis of DNA replication timing reveals conserved large-scale chromosomal architecture. PLoS genetics *6*, e1001011.

Zhou, T., Georgiev, I., Wu, X., Yang, Z.Y., Dai, K., Finzi, A., Kwon, Y.D., Scheid, J.F., Shi, W., Xu, L.*, et al.* (2010). Structural basis for broad and potent neutralization of HIV-1 by antibody VRC01. Science *329*, 811-817.

Zikherman, J., Parameswaran, R., and Weiss, A. (2012). Endogenous antigen tunes the responsiveness of naive B cells but not T cells. Nature *489*, 160-164.